Regional Climate Change: The Role of Light-Absorbing Aerosols and Snow-Albedo Feedback

Distinguished Lecturer in Atmospheric Sciences: Asia Oceania Geosciences Society (AOGS) 8th Annual Meeting, August 9, 2011, Taipei, Taiwan

Kuo-Nan Liou, University of California, Los Angeles, CA, USA

Mr. Chairman and distinguished colleagues, I am pleased to have the opportunity to attend the AOGS 8th Annual Meeting held in Taipei. First, I would like to thank our chair Professor Chun-Chieh Wu of National Taiwan University and the organizer for the invitation.

*** My talk is concerned with regional climate change with a focus on the issues of 3D mountain/snow and absorbing aerosols as a regional climate system. In particular, I would like to share with you my perspective on the importance of absorbing aerosols, specifically black carbon (BC) and dust particles, in the reduction of snow albedo vis-a-vis aerosols-mountain snow-albedo feedback that has an irreversible impact on regional climate and climate change (Slide 1).**

*** For your enjoyment, I have selected a number of slides (Slides 2-7) to illustrate the retreat of mountain snow in a number of locations, including the Kyetrak and Rongbuk Glaciers in Tibet, China; Mount Kilimanjaro in Tanzania; the Qori Kalis Glacier in Peru; and the Grinnell Glacier of Glacier National Park and the South Cascade glacier of Washington State in the United States. It appears quite evident that the reduction of mountain snow fields over the globe must be related to global warming. However, I submit that the addition of man-made (or anthropogenic) absorbing aerosols must also play a substantial role in this reduction in a non-linear fashion.**

*** The global reduction of snow field can also be seen from Slide 8 taken from IPCC (2007). Panel (a) illustrates the NH March-April snow covered area obtained from ground-based and NOAA satellite datasets. The smooth curve shows decadal variations. Panel (b) shows differences in the distribution of NH M-A average snow cover between earlier (1967-1987) and later (1988-2004) portions of the satellite era. Yellow colors represent the reduction of snow cover. And I have selected two specific areas: the Tibetan Plateau and**

the Sierras in the northern California-Nevada, for my presentation. The Tibetan Plateau, with its mighty mountains, is considered to be the third pole of the Earth because of the area of snow cover. The Sierra Nevada Mountains have substantial snow events in the winter and spring, representing important water resources not only for northern but also southern California. In fact, about 45% of S.C. water resources come from the Sierras.

*** With respect to the Tibetan Plateau, Slide 9 illustrates the BC concentration determined at the Zuoqiupu Glacier from 1955-2005. Shown are annual and 5-year running mean results for monsoon, non-monsoon, and annual cases. The source of BC is primarily from the Indian subcontinent. Also shown in the middle and lower panels are corresponding surface air temperature and snow accumulation, respectively. It appears to demonstrate that the reduction in snow in that area is related to surface air temperature, as well as an increase in BC.**

*** Slide 10 displays the BC (soot) concentration measured during the INDOX experiment, which was conducted in March 2001. The biomass burning in Southeast Asia and India have been identified and recognized as regions of important sources.**

*** Slide 11 shows the dust originating in East Asia and China, as demonstrated in the 2001 perfect dust storm, using the aerosol optical depths determined from the TOMS instrument on board NOAA satellites to display the cross-Pacific transport of dust particles.**

*** In order to understand the transport of BC/dust aerosols from East Asia to the United States, we have analyzed the aerosol optical depths available for MODIS/NASA over the Sierra-Nevada Mountains, a region with snow cover in the winter season, for March and April, during a 9-year period. These results (Slide 12, only 4 years are shown) clearly illustrate the cross-Pacific transport of aerosols in general and BC/dust in particular from East Asia (source regions, red/yellow, 0.7 – 1 optical depths) to the Sierra-Nevada Mountains (green/light yellow, 0.3-0.5 optical depths). The selection of March-April is related to the aerosol activities in East Asia and the issue of snowmelt and water resources in California.**

*** In addition, we have run a simulation using a chemical transport model,**

referred to as GEOCHEM. This simulation (Slide 13) was conducted for the total aerosol optical depth in March and April for the year 2006; the results of this simulation reinforce the previous satellite aerosol optical depth observations. We need a chemical/aerosol transport model in order to quantify wet and dry depositions of absorbing aerosols onto the snow fields, a subject we are currently working on.

*** Over the Sierras, local emissions from industrial sites represent the major sources of BC (~ 70%) that were observed. For illustration purposes, I have selected local sources using Los Angeles air pollution and the air pollution produced in Northern California as examples (Slide 14).**

*** Slide 15 displays a snow scene over the Sierra-Nevada Mountains in Northern California regions.**

*** I wanted to demonstrate that the lower snow albedo values in April compared to those in March are in part caused by absorbing aerosols transported from China and Southeast Asia. For this purpose, we analyzed the monthly mean and standard deviation of snow albedo (ranging from 0.5-0.8, Slide 16) and aerosol optical depth based on satellite observations. We show that the snow albedo in April is consistently lower than in March, whereas the reverse is true for aerosol optical depth. Correlation analysis shows that these two parameters are negatively correlated with a high correlation coefficient and are statistically significant. I fully realize that snow albedo is also correlated with surface temperature in which the month of April is generally warmer than the month of March, as well as the precipitation event, in terms of the days after the snowfall. Nevertheless, I would argue that the decrease in snow albedo with 100% snow cover in April, as compared with March is in part caused by the effect of absorbing BC and dust from East Asia. Of course, additional research needs to be done to confirm this finding.**

*** Slide 17 presents a summary of the sources of BC and dust from China and Southeast Asia. First on BC, China is a significant source of BC production, particularly in recent years. BC is produced by the incomplete combustion of carbonaceous fuels, including fossil fuel and biomass burning. China has been recognized as a major global anthropogenic source for BC aerosols. Coal production during the 1990s was 5 times larger than during the 1960s. About**

10% of global carbon emissions in 1990 came from China and this value increased to 12 % in 2000. A projection to 2025 indicated that it would be increased to 18%. In addition to the preceding sources, biomass burning in Southeast Asia and Indian subcontinent has also been recognized as a substantial source of the production of BC. With reference to dust, these particles originate in northwest China (the Gobi Desert, Taklamakan Desert, and Tarim basin area) in late March and early April associated with special weather conditions, resulting in extremely dry areas with precipitation less than 200mm. Dust production is directly related to regional weather systems, however, it can also be indirectly generated by man-made perturbations, such as deforestation and desertification.

*** Dust particles are nonspherical and scatter and absorb sunlight, making the determination of their single-scattering properties a difficult issue in radiative transfer and remote sensing. Soot or BC particles are more complicated and some of them have fractal structures with respect to their morphology and composition (Slide 18). Soot is an aggregation of individual monomers, which can be structured in terms of internal and external mixing resulting in open and closed clusters or aggregations. These configurations lead to significant differences in their optical properties and the consequent single-scattering albedo value, a ratio of scattering to extinction cross sections, important in climate study. I will demonstrate this point in a later slide in conjunction with their interaction with snow grains.**

*** Why are BC and dust particles important in global radiative forcing and the climate system? The first reason is related to their direct radiative interactions with sunlight. The direct radiative forcing of BC/dust is determined by absorption and scattering processes and I have illustrated the physical connection of atmospheric absorption to vertical temperature profile, regional circulation, and regional surface temperature and precipitation on the right of this slide (Slide 19).**

*** Slide 20: GCM simulations and comparison with observations to illustrate the significance of BC concentrations and the associated single-scattering albedo on the simulations of surface air temperature and precipitation over China. BCs are assumed to be spherical and external mixing and internal**

mixing states have not been accounted for in the single-scattering calculations.

*** Slide 21: In order to have a fundamental understanding of the radiative properties of BC, we must consider its basic geometric structure, size, composition, and optical properties. I shall now confine my presentation to radiative transfer in aerosols and focus on black carbon. Soot or BC particles are complex with regards to their size, morphology, and composition. They are aggregations of individual monomers, which can be structured in terms of internal and external mixing resulting in open and closed clusters, leading to substantial differences in their absorption and scattering properties, critically important in climate study. We have recently developed a new theoretical approach, which combines a stochastic process to build aggregates, followed by the geometric photon tracing including reflection/refraction, diffraction, and surface waves. The building block can be homogeneous or coated spheres with smooth or rough surfaces. We show an example of the stochastic process to construct aggregates that resemble their observed shape in the air. The light absorption and scattering program by small irregular particles based on the geometric-optics and surface-wave approach has been verified by comparison with existing results for columns and plates. The next 3 slides show some representative results.**

*** Slide 22 illustrates substantial differences between realistic aggregate shapes and commonly assumed spheres in terms of reflection, absorption, and transmission for typical BC sizes of 0.03 (and 0.07 μm) as a function of aerosol mass path. Because of irregular shapes, the optical depth can be determined from mass extinction coefficient and aerosol mass path. Aggregates reflect and absorb more than their spherical counterpart. Spheres are not a good approximation for BC in radiative transfer calculations.**

*** Slide 23: In the following slide, we illustrate the importance of the contamination of snow grains by absorbing aerosols. Internal mixing produces much larger absorption, as compared with its external counterpart, in terms of a larger single-scattering co-albedo. The subsequent radiative transfer calculations illustrate reduction of snow albedo associated with the contamination of BC and dust particles, depending on their size. Due to its**

larger absorption, BC has a more substantial impact than dust particles do on the reduction of snow albedo. A 1-□m sized soot particle internally mixed with snow grains could effectively reduce snow albedo by as much as 5-10 %.

*** Slide 24: Spectral snow albedo results for snow grains externally and internally mixed with 3 sizes of soot particles to illustrate the importance of internal mixing in snow grains in the reduction of snow albedo. The information content is quite rich at the fundamental level; however, in the interest of time I shall move to 3D radiative transfer in mountains/snow.**

*** Slide 25: It appears unlikely that analytical solutions, such as 2-stream, Eddington, and 4-stream approximations for radiative transfer, can be derived for intricate mountains/snow fields. In my opinion, the only solution is by means of the Monte Carlo simulation, which can be applied to any geometry, but unfortunately, formidable computational efforts are required to achieve reliable accuracy. We have made significant advances in modeling the transfer of solar and thermal IR radiation involving intense topography following Monte Carlo photon tracing. The transfer of solar radiation is composed of 5 components- direct, diffuse, direct-reflected, diffuse-reflected, and coupled fluxes- related to the solar incident angle, elevation, sky view factor, and terrain configuration factor.**

*** The following Slide (26) illustrates differences between the domain-averaged net radiative flux on mountains and a flat surface as a function of the time of day using two domains of 30 and 50 km (centered at Lhasa, Tibet) on March 21 (equinox). In reference to a flat surface, 3D mountain effects can produce about 10-30 W/m^2 differences in solar fluxes in a regional scale of 30 km domains. Longwave radiation only shows differences less than 5 W/m^2. The radiation flux component of 10-30 W/m^2 is indeed substantial and must be accounted for in the evaluation of surface temperature perturbation, especially over snow surfaces.**

*** This Slide (27) displays a comparison of the deviations (from plane-parallel results) of the five flux components computed from Monte Carlo simulations (real values) and multiple regression equations (predicted values) using a domain of 10 km. The upper panel is for direct and diffuse fluxes. The middle panel is for direct-reflected and diffuse-reflected fluxes. The lower**

panel shows the coupled flux with a surface albedo of 0.1 and 0.7. The most important component is direct flux (~ 700 W/m^2), followed by direct-reflected flux. We have derived 5 universal regression equations for flux deviations which have the general linear form for the 5 flux components, as shown in the lower panel. For example, for the deviation of direct flux, F^*_{dir}, we have $a_1 + b_{11}\, y_1 + b_{12}\, y_2$, where y_1 is the mean cosine of the solar zenith angle, y_2 is the mean sky view factor, and b_{11} and b_{12} are regression coefficients. This parameterization is applicable to clear as well as cloudy conditions using cloud optical depth as a scaling factor. The flux deviation results can be directly added to the existing surface flux values determined from a land-surface model to account for 3D mountain effects. I would like to point out that the original idea of using deviations in the parameterization was due to Dr. Wei-Liang Lee of the Academia Sinica.

*** Our research is now supported by the National Science Foundation and Department of Energy to pursue regional climate modeling with the inclusion of two first principles; namely, 3D radiative transfer in mountains/snow and radiative transfer in absorbing aerosols. Our conceptual approach is illustrated in Slide 28, which displays a graphic depiction of the effect of 3D mountain/snow and absorbing aerosols with respect to the solar inputs as a combined regional climate system.**

*** Slide 29 demonstrates the essence of snow-albedo feedback, a powerful amplification process involving absorbing aerosols. Through the wet and/or direct dry deposition of absorbing aerosols, snow becomes less bright. As a consequence, it will absorb more incoming sunlight, which will lead to surface warming. The loop involving darker snow and absorbing more sunlight forms a powerful feedback that can significantly amplify increase in surface temperature. In this conjunction, we have witnessed powerful ice-albedo feedback in the Arctic and Antarctic regions. However, we need to quantify the surface warming produced by dry and wet depositions. Also, we do not know the 3D mountain radiative effect in a model setting on the state of snow albedo with reference to the conventional plane-parallel radiative transfer program.**

*** The next slide (Slide 30) illustrates the global radiative forcings**

produced by natural and human disturbances of climate change, including greenhouse gases, aerosols, and other forcing elements. Globally, BC on snow is shown to have only a small value; without question, however, this forcing must be much more substantial in the regional context, particularly if the powerful feedback processes have been properly included and accounted for.

*** We are now in the process of incorporating the 3D radiative transfer parameterization in the CLM developed at NCAR, which will be linked to WRF (Slide 31). The 3D mountain/snow effect on radiation field will be in solar insolation terms in the surface energy balance system equation. We are also preparing the single-scattering properties of BC for incorporation into the CLM snow model for sensitivity studies involving snow grains internally and externally mixed with BC.**

*** In the last slide (Slide 32), we present a summary of the impacts of climate change, including global warming produced by greenhouse gases and the effects of absorbing aerosols on snow albedo on the climate of California with reference to a number of key surface climate parameters, including (1) precipitation and snow distribution related to mountain ecosystems and the ski industry, (2) water resources and management, (3) Santa Ana wind events affecting human health and wildfire, (4) runoff and streamflow associated with coastal wetlands, and (5) sea surface temperature pertinent to ocean ecosystems. Indeed, the State of California is particularly vulnerable to global warming and climate change.**

*** In conjunction with the last bullet point, we at the Joint Institute for Regional Earth System Science and Engineering have been working on building a Regional Climate Model to include two new physical processes: parameterization of 3D radiative transfer in mountains/snow field for incorporation in the Weather Research Forecast (WRF) model and the Community Land Model (CLM); and investigating the impacts of size, shape and composition of soot on solar radiative forcings in terms of the states of external/internal mixing and their interactions with snow grains.**

On this note, let me conclude my presentation. Thank you very much for your attention.

Regional Climate Change: The Role of Light-Absorbing Aerosols and Snow-Albedo Feedback

***Kuo-Nan Liou**
Joint Institute for Regional Earth System Science and Engineering (JIFRESSE) and Atmospheric and Oceanic Sciences Department
University of California, Los Angeles, CA, USA

***With contributions from W. L. Lee, Y. Takano, Y. Gu, Q. Li, R. Leung, P. Yang, and T. Fickle. Research work supported in part by NSF and DOE.**

- **Evidence of Mountain Snowmelt and Climate Change**
- **BC and Snow Cover Reduction in the Tibetan Plateau**
- **Some Evidence of Snow Albedo Reduction in the Sierras**
- **Radiative Forcing by BCs (Aggregates)**
- **3D Mountain/Snow and the Concept of Absorbing Aerosols - Snow-Albedo Feedback**
- **Connection to the Community Land Model (CLM) and WRF, and Summary**

Asia Oceania Geosciences Society 8th Annual Meeting, Taipei, August 9, 2011

Kyetrak Glacier, Tibet

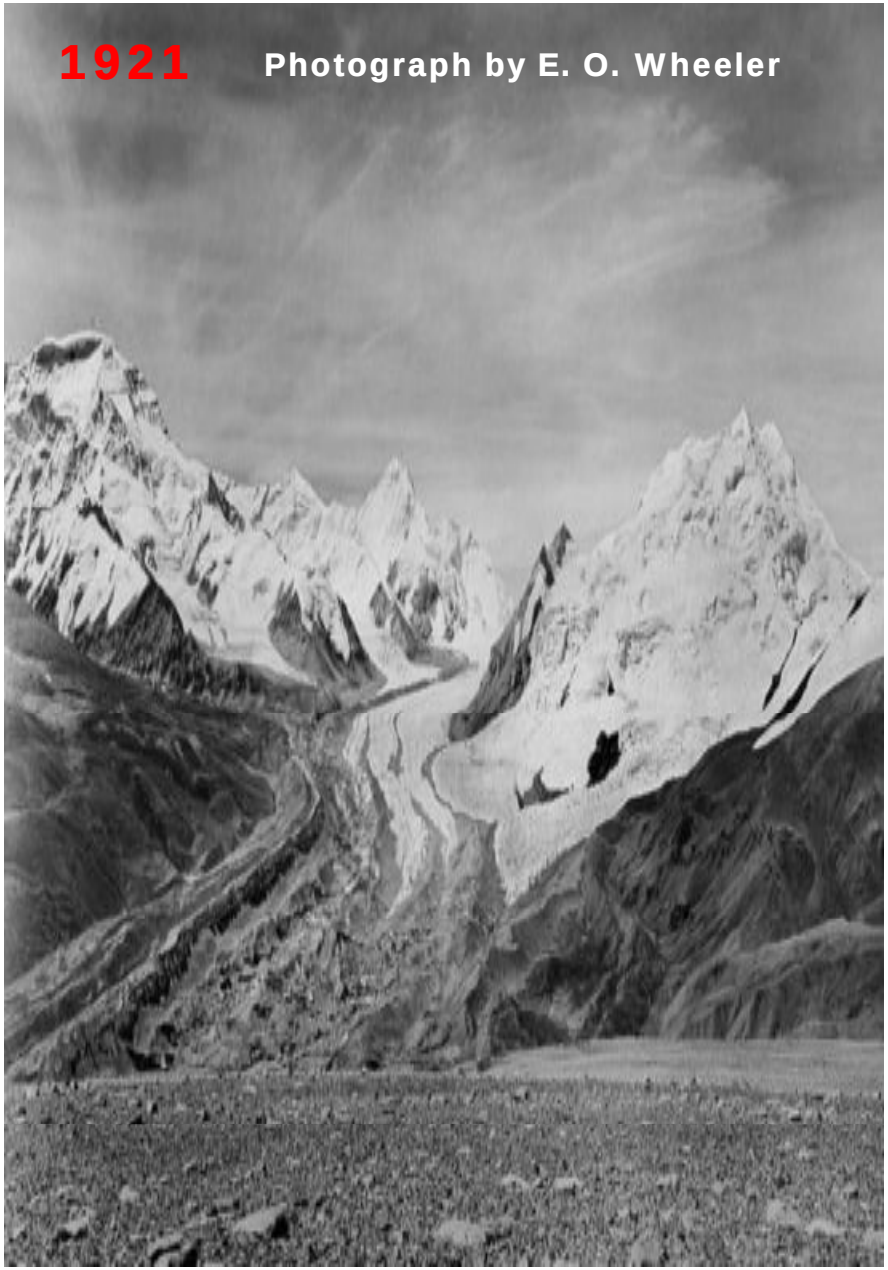

Rongbuk Glacier, Tibet

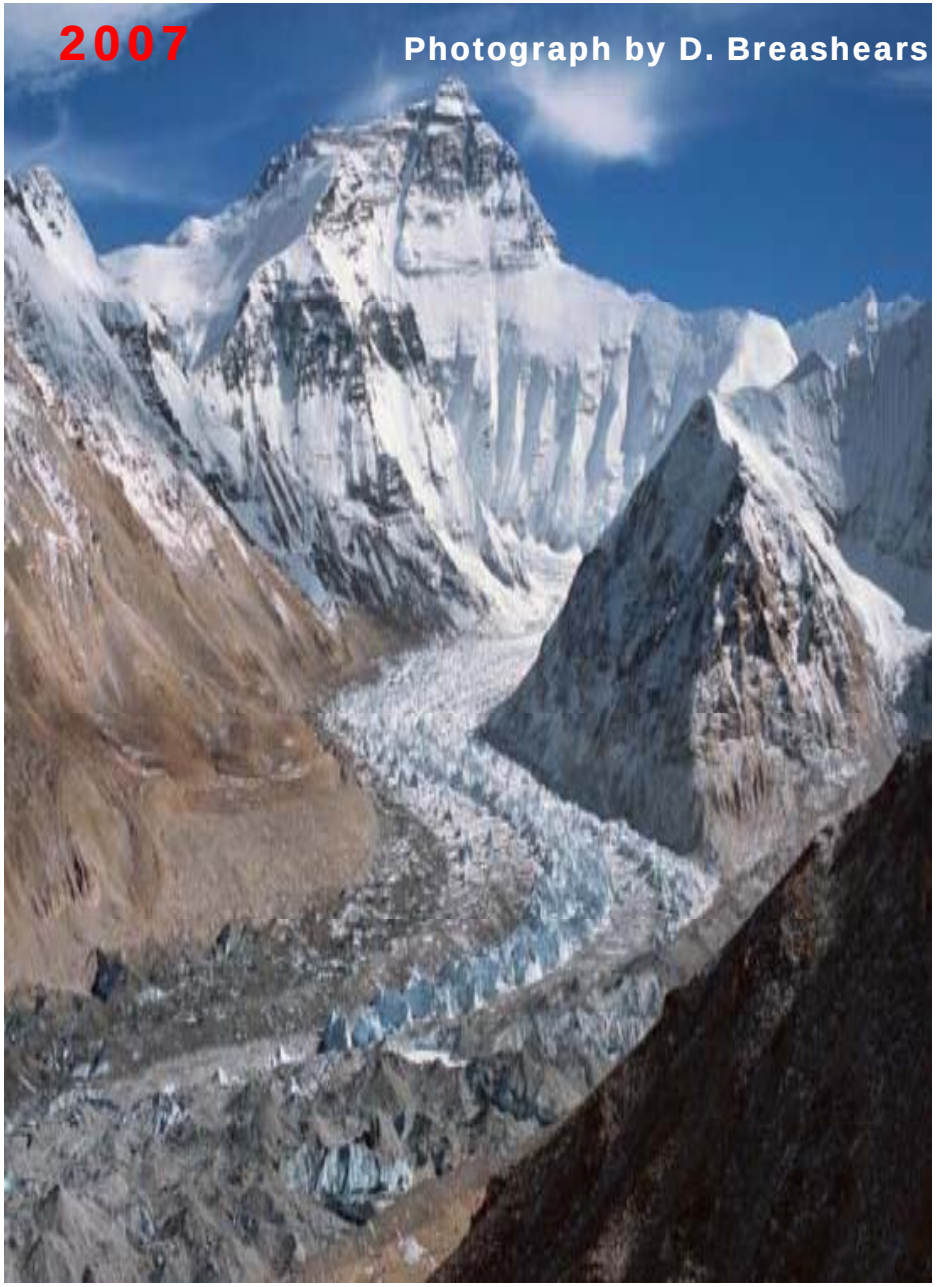

Mount Kilimanjaro, Tanzania

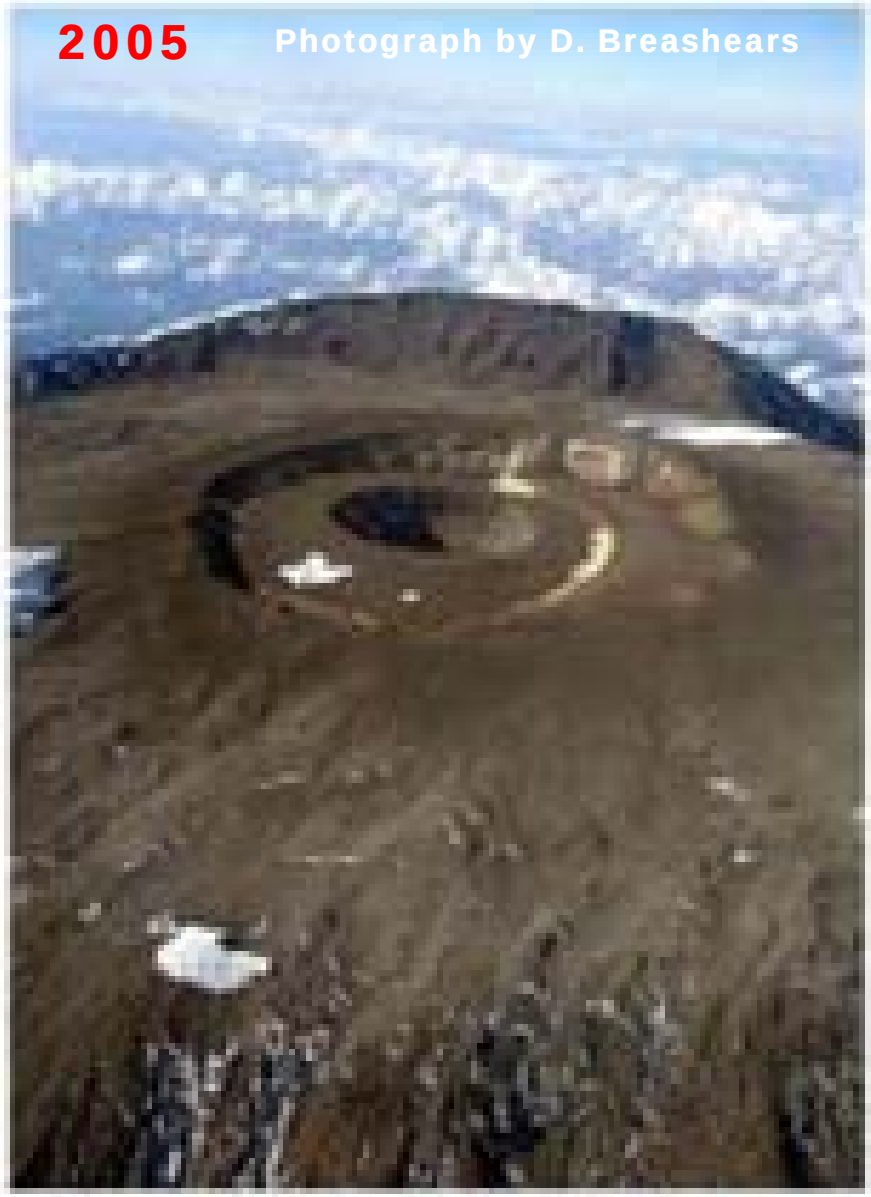

Qori Kalis Glacier, Peru (World Data center for Glaciology)

Grinnell Glacier, Glacier National Park

Strong Evidence for Global Warming; however, absorbing aerosols have also contributed to and amplified the retreat of glaciers.

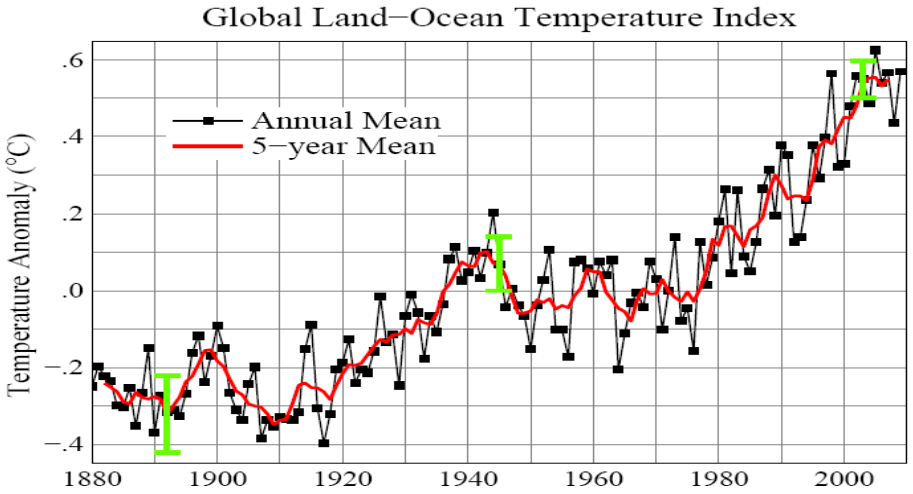

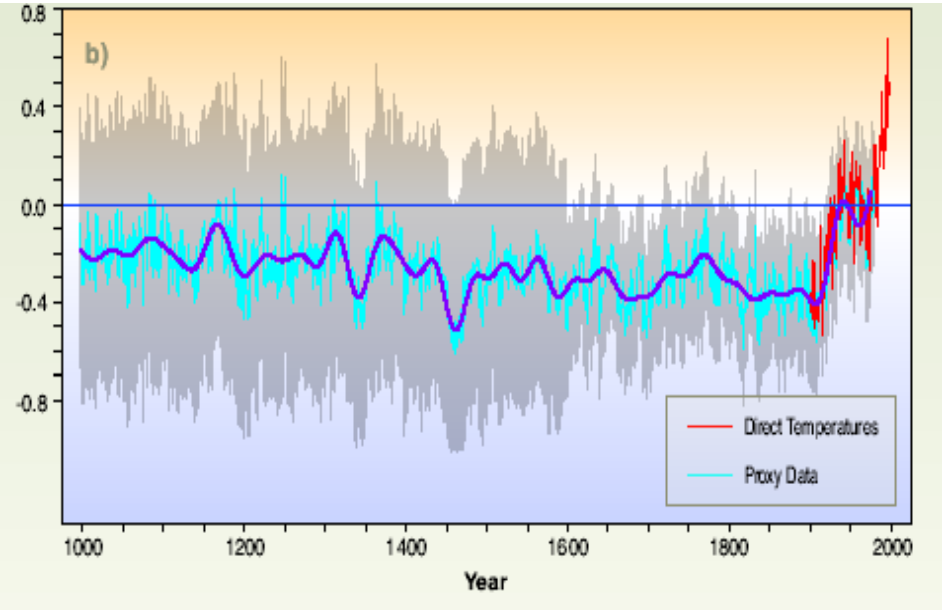

Sources: James Hansen and IPCC 2001 Report

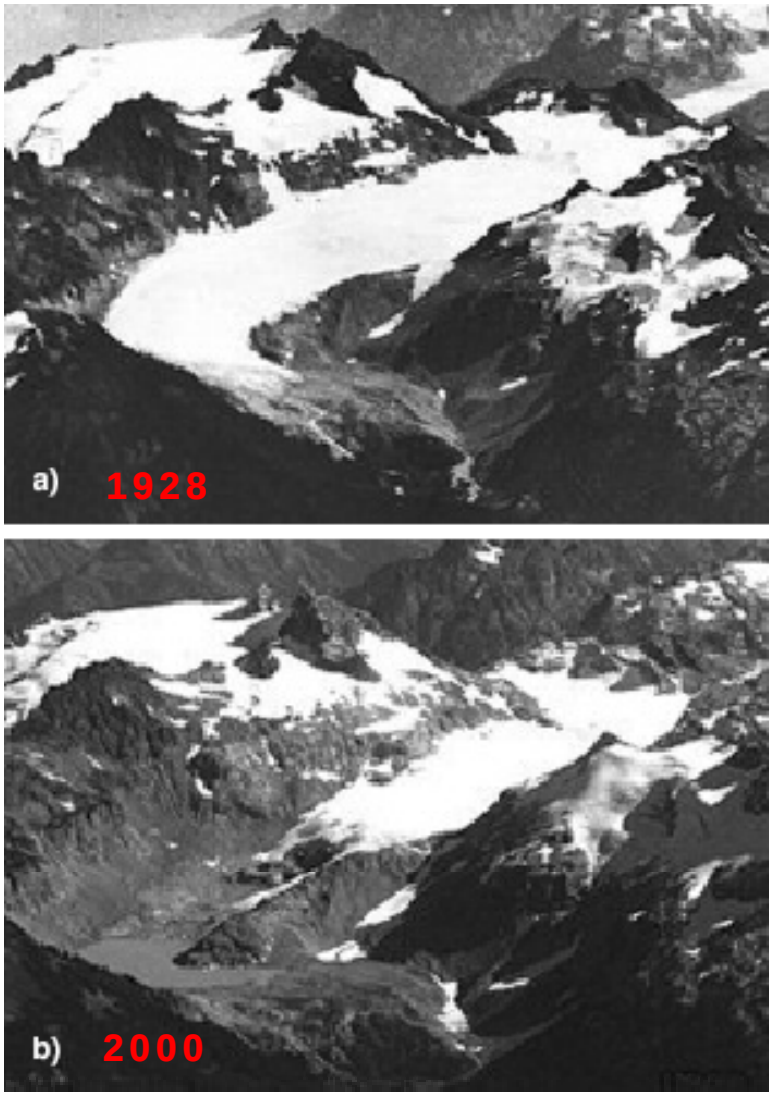

South Cascade Glacier, Washington (US Geological Survey)

(a) NH March-April average snow-covered area (Brown 2000) and NOAA satellite data set. The smooth curve shows decadal variations, and the shaded area shows the 5 to 95% range of the data estimated after first subtracting the smooth curve. (b) Differences in the distribution of NH March-April average snow cover between earlier (1967–1987) and later (1988–2004) portions of the satellite era. Negative values indicate greater extent in the earlier portion of the record. Red curves show the 0 and 5^0 C isotherms averaged for March and April 1967 to 2004 (after IPCC 2007).

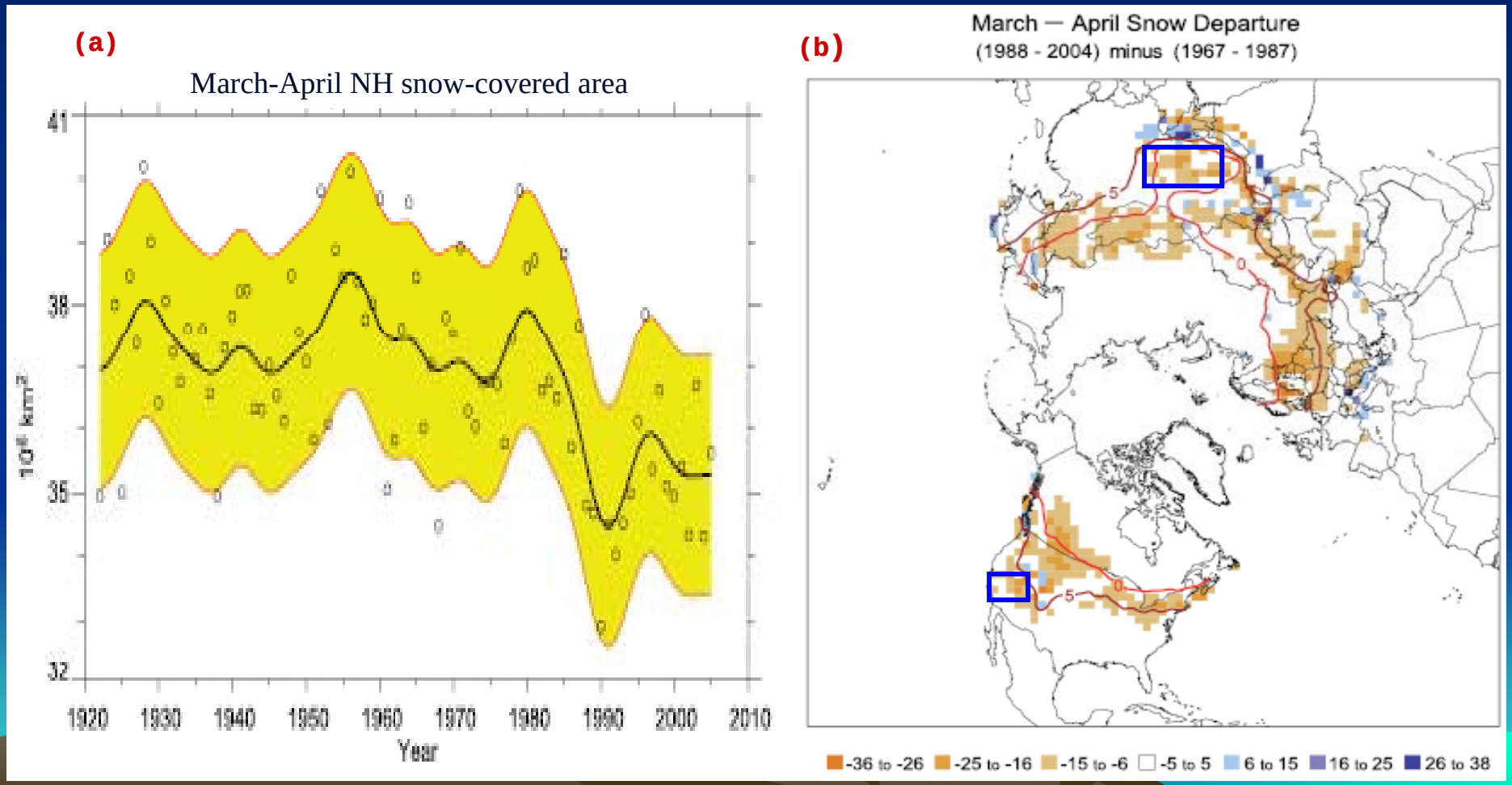

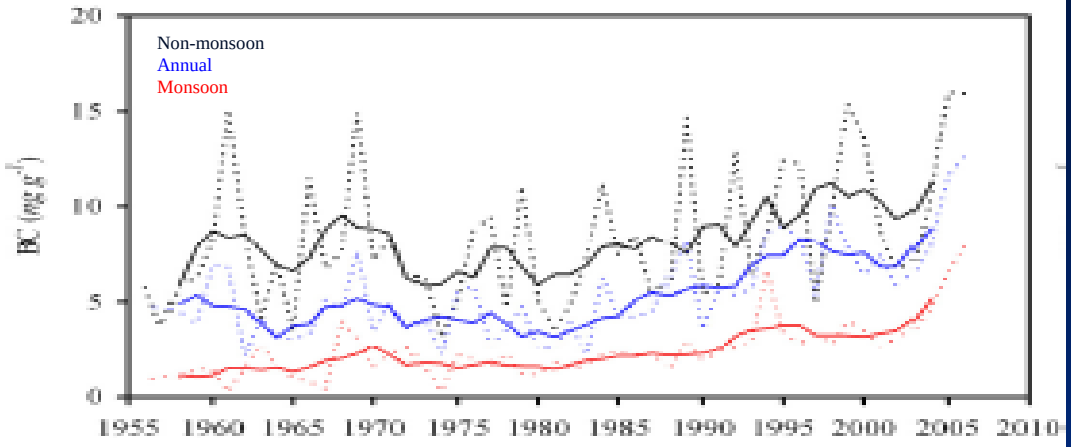

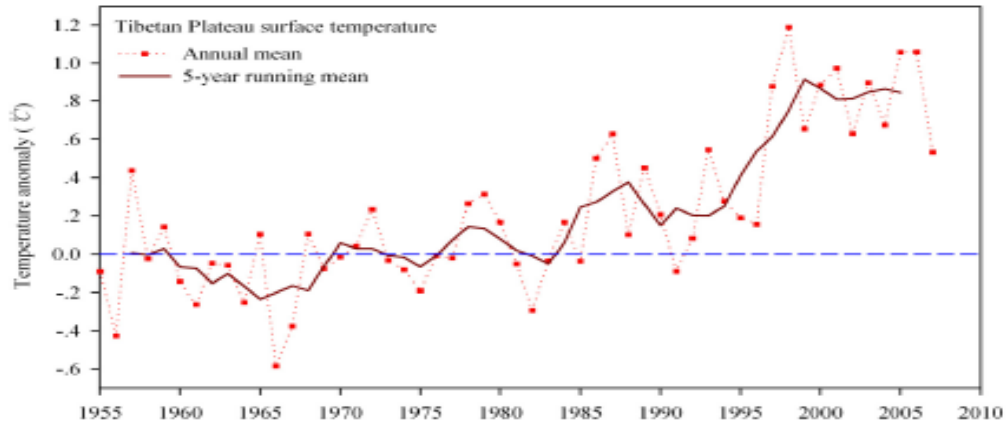

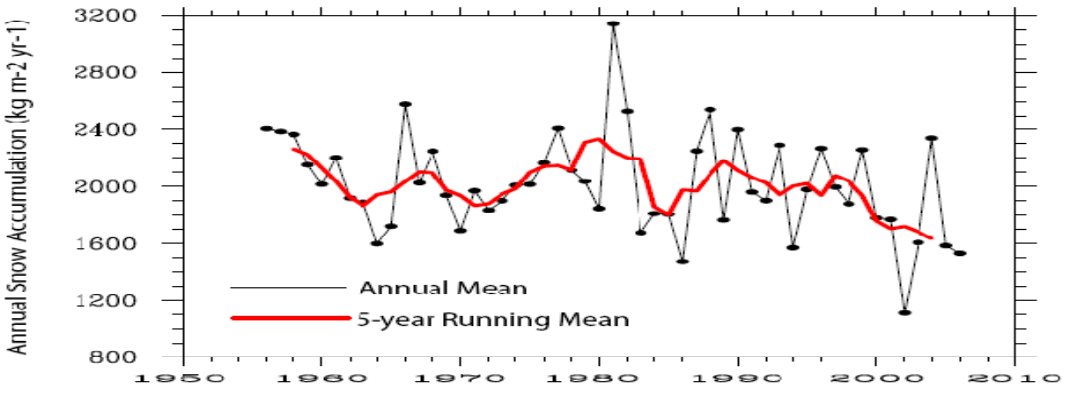

Top: Black carbon concentration (ng/g) determined at the Zuoqiupu Glacier of the Tibetan Plateau from 1955 to 2005. Shown are annual and 5-year running mean results for non-monsoon, monsoon (lower due to high precipitation rate), and annual cases. The BC source is Asia, primarily the Indian subcontinent.

Middle: Surface air temperature anomaly in terms of annual and 5-year mean on the Tibetan Plateau relative to 1951-1980 mean, averaged over the area with altitude greater than 4,000 m above sea level.

Bottom: Annual snow accumulation on the Zuoqiupu Glacier (kg/m2/yr) from 1956 to 2006 along with 5-year running mean results, revealing reduction since 1990 (after Xu et al. 2009).

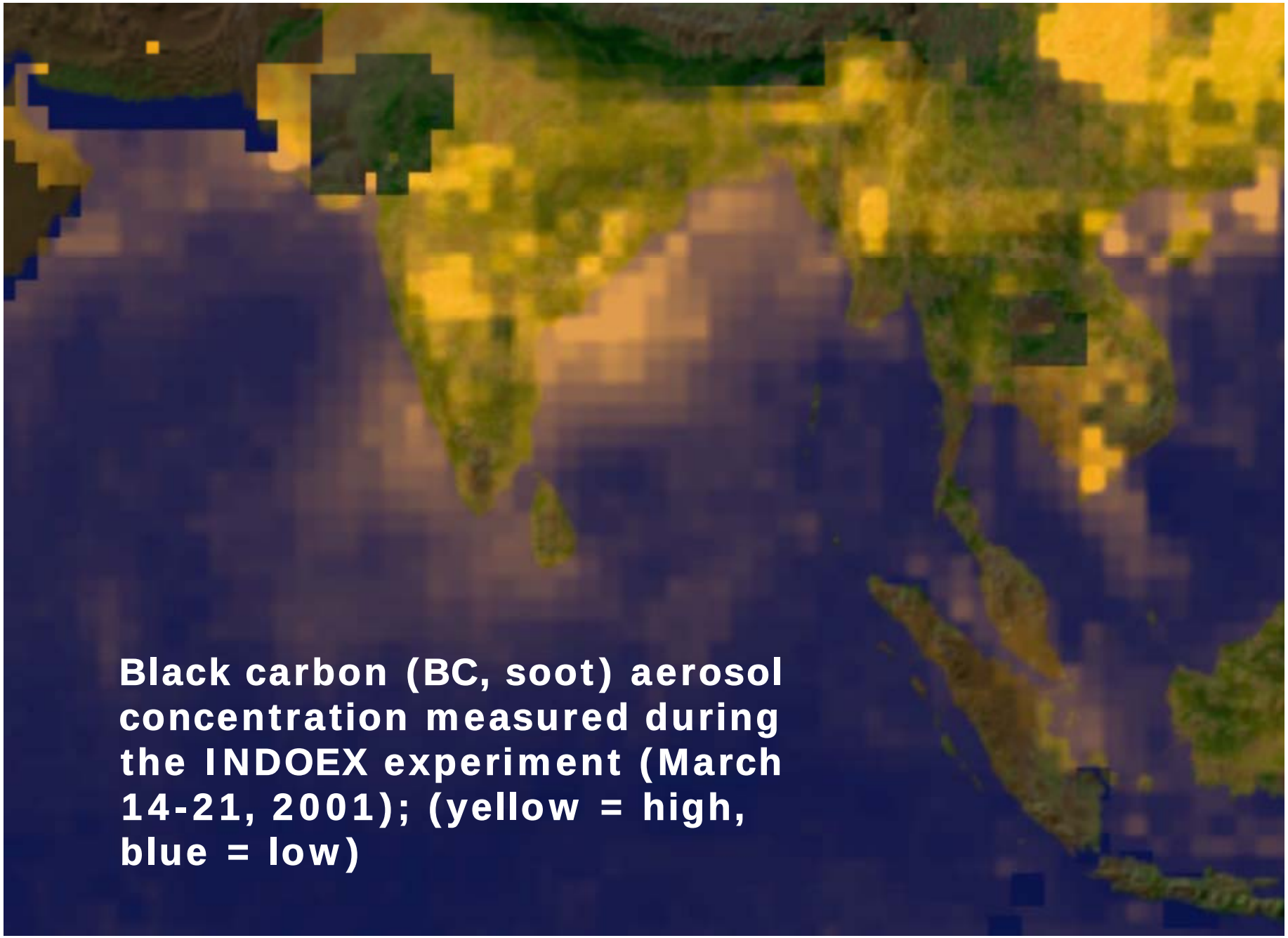

Black carbon (BC, soot) aerosol concentration measured during the INDOEX experiment (March 14-21, 2001); (yellow = high, blue = low)

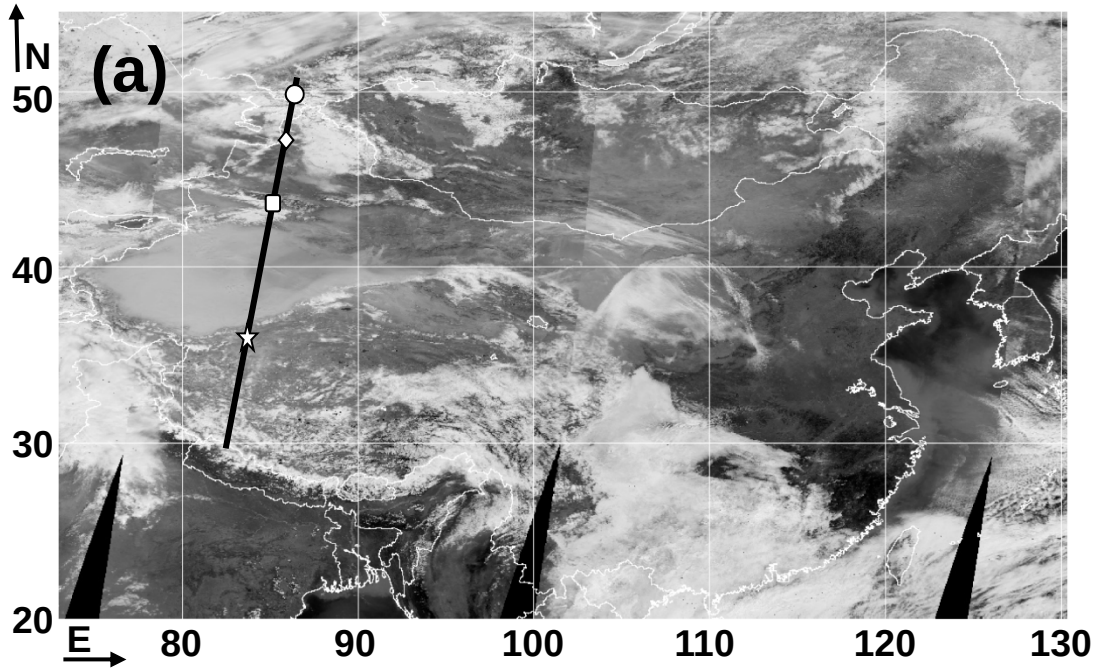

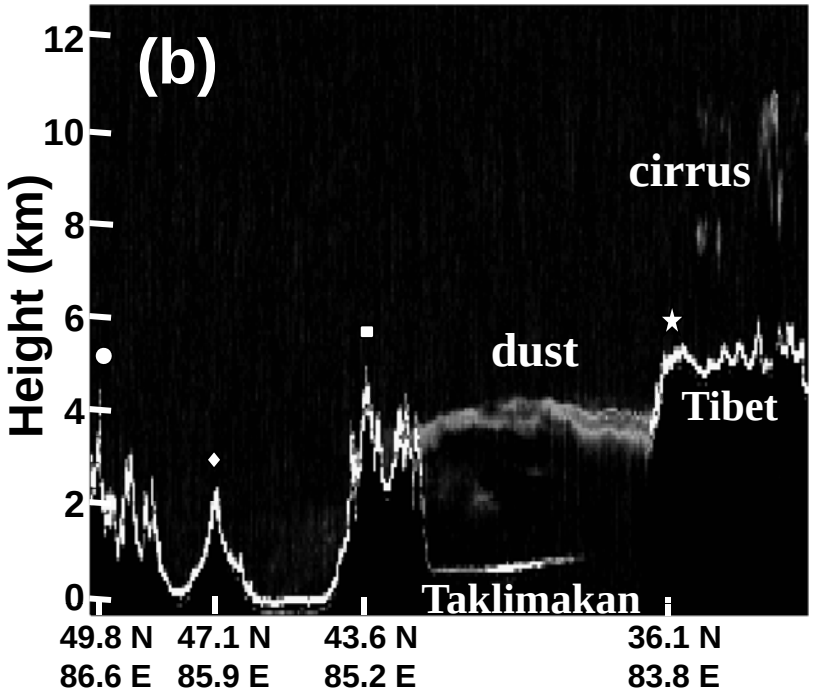

(After Tsay et al. 2008)

"2001 Perfect Dust Storm"

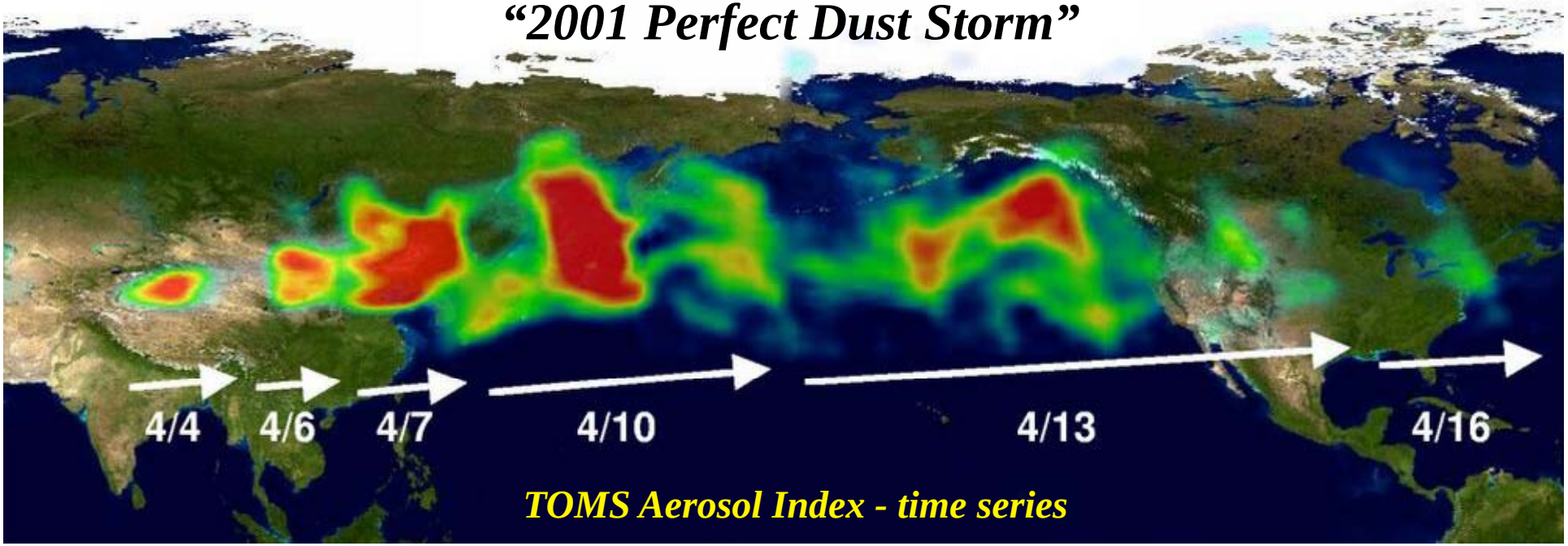

TOMS Aerosol Index - time series

Aerosol optical depths determined from MODIS of NASA satellites for March and April 2000-2009, a 10 year period, illustrating the transport of absorbing aerosols from China and Southeast Asia across the Pacific to the United States (only 4 years are shown; courtesy of W. L. Li, Academia Sinica).

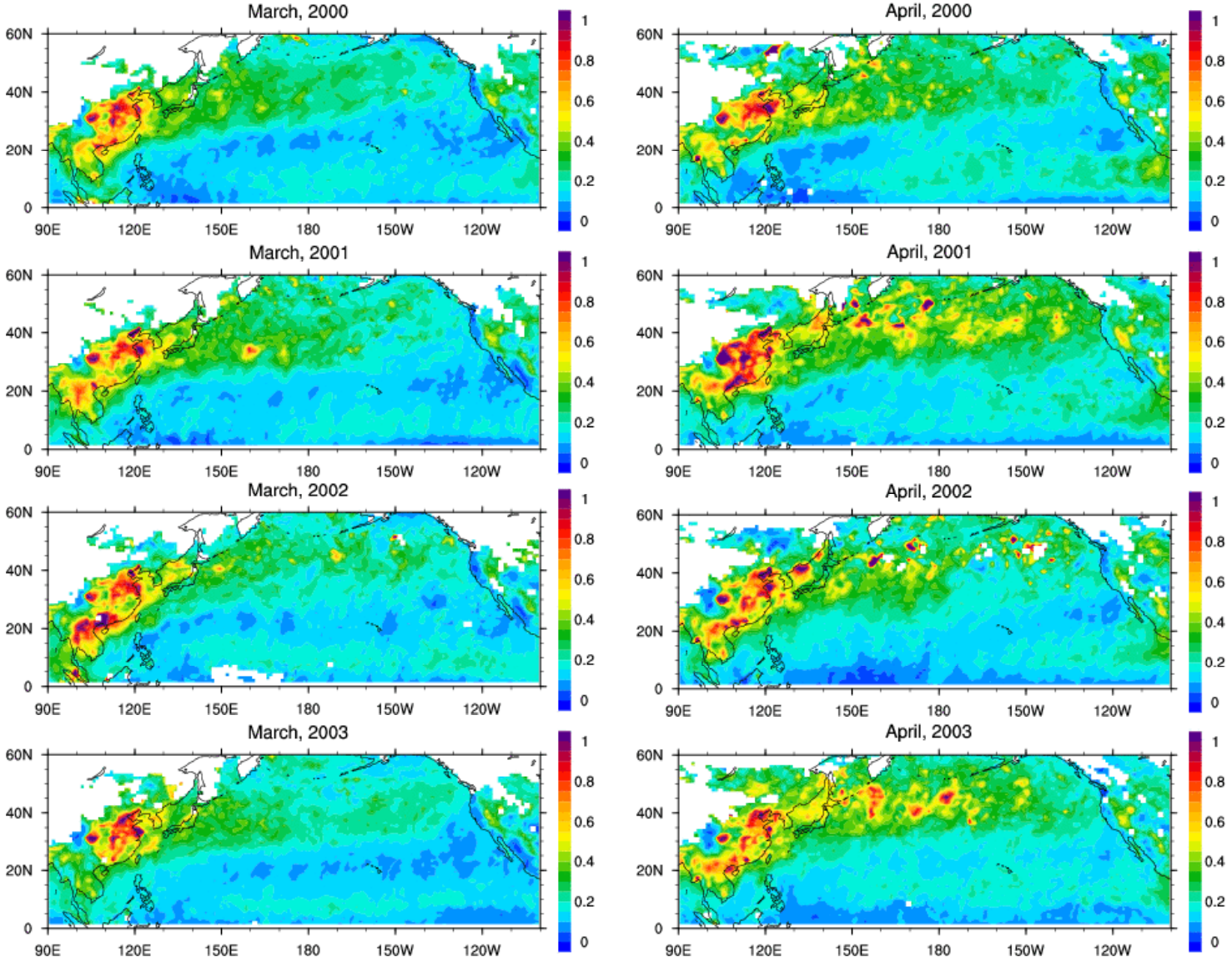

Total aerosol optical depths for March and April 2006 simulated from a chemical transport model, illustrating the effects of absorbing aerosols generated in China on the west coast of the United States (courtesy of Q. Li, UCLA).

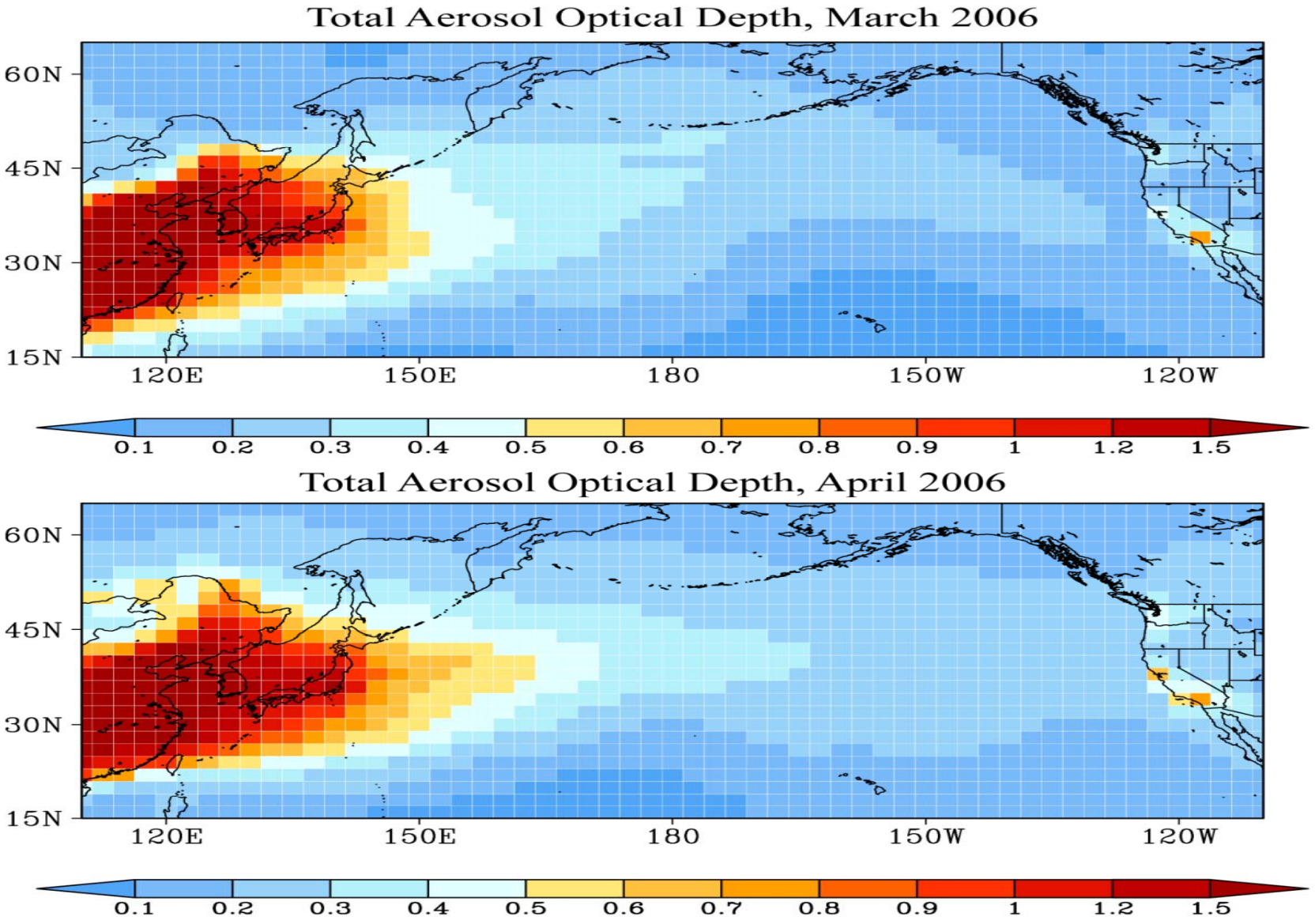


Northern California (local)
Southern California (local)

Sierra Nevada Mountains:
BC/Dust-Snow Impact on Regional Climate

Monthly averages of snow albedo, land surface temperature, and days after each snowfall event for pixels with 100% snow cover, and aerosol optical depth over the Sierras in March and April from 2000 to 2009. Error bars indicate one standard deviation: $\alpha = 0.56\text{-}0.038T\text{-}0.026\tau$ (Lee and Liou 2011).

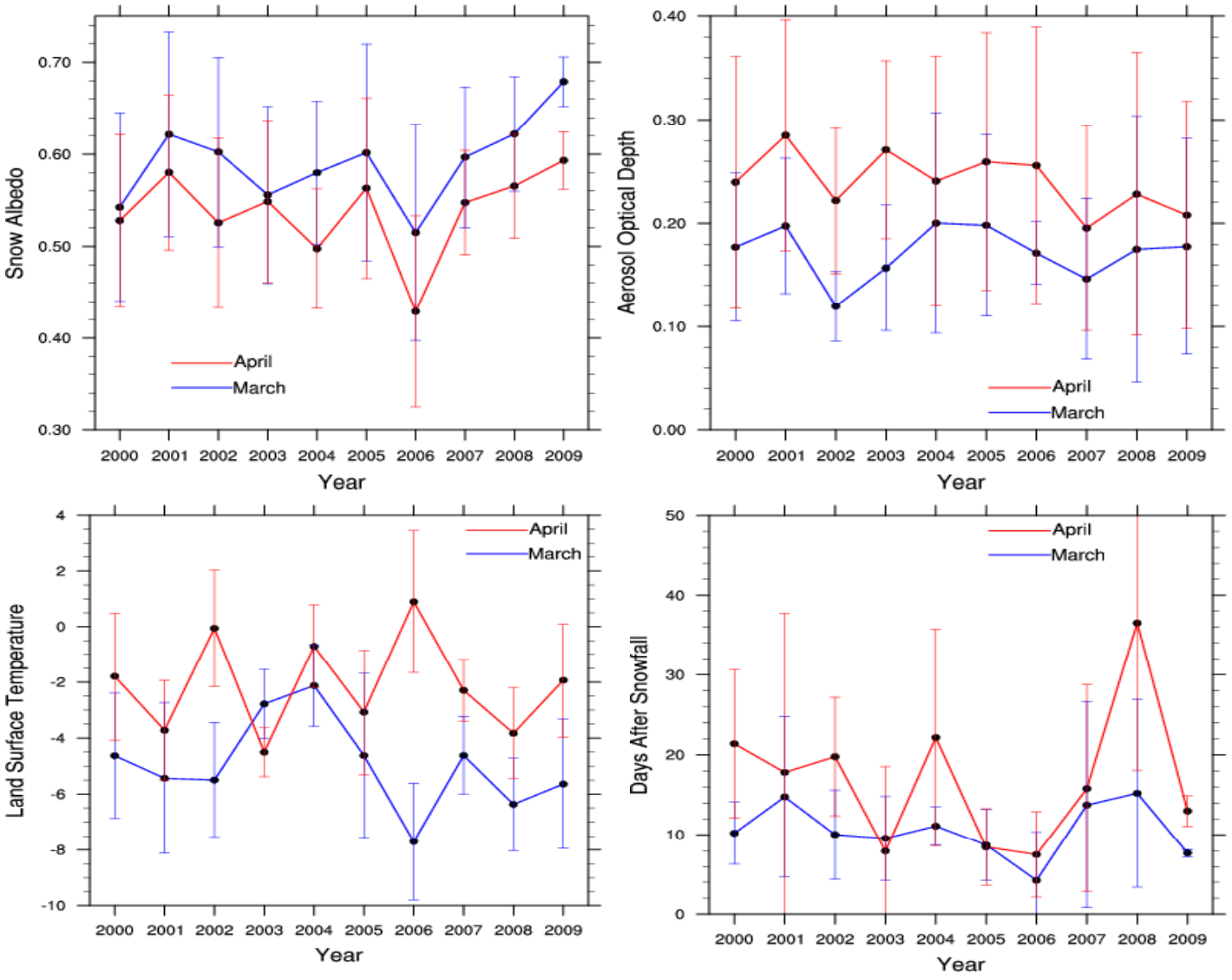

Asian Sources of BC and Dust Particles

- **BC:** Incomplete combustion of carbonaceous fuels, including fossil fuel and biomass burning
  - China: 80% of energy comes from coal combustion
    Recognized as a major global anthropogenic source for BC aerosols: Coal production during the 1990s was 5 times larger than that during the 1960s
    ~10% of the global carbon emission in 1990
    ~12% in 2000
    ~18% in 2025 (projection)
  - Southeast Asia & Indian subcontinent: Biomass burning
- **Dust:** Originating in northwestern China (Gobi Desert, Taklamakan Desert, and Tarim basin area) in late March and early April (extremely dry areas < 200mm precipitation, and special weather conditions)

Light Scattering and Absorption by Dust and Black Carbon: Fundamental to the Understanding of Aerosol Climate Forcings

Dust

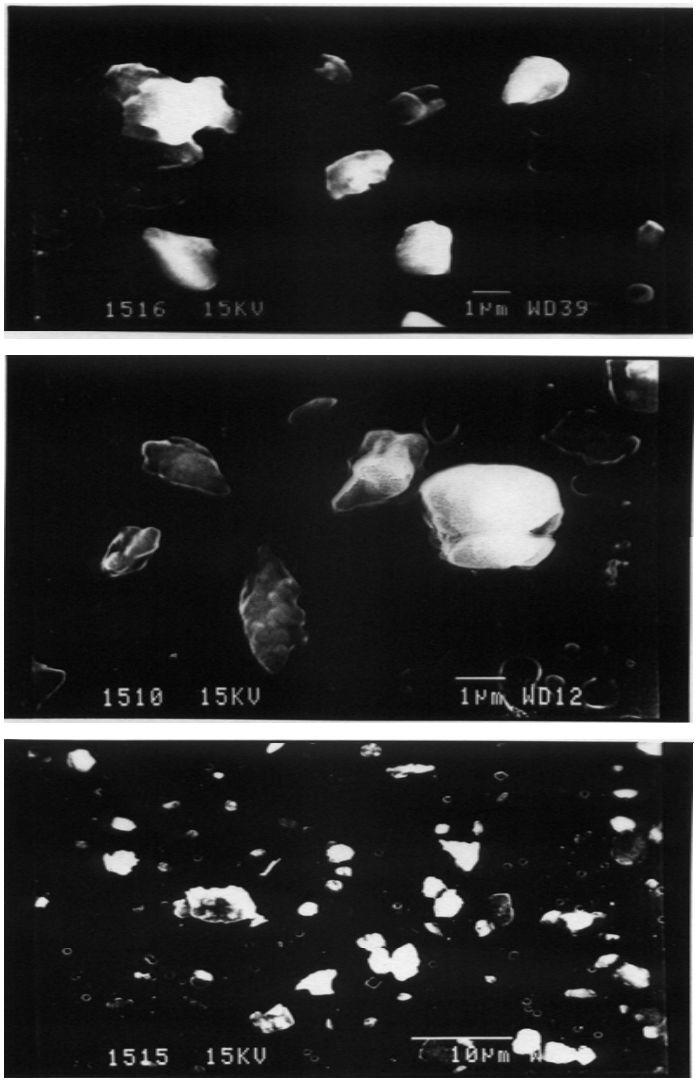

Black Carbon

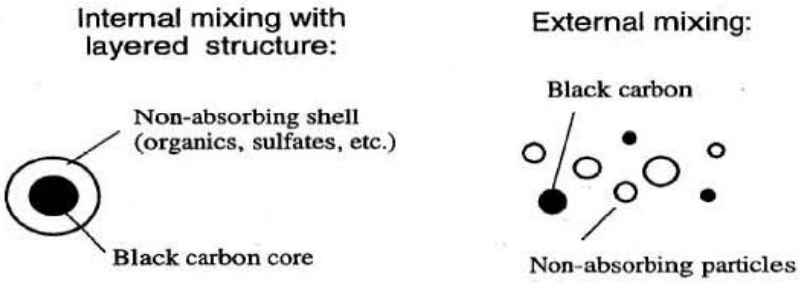

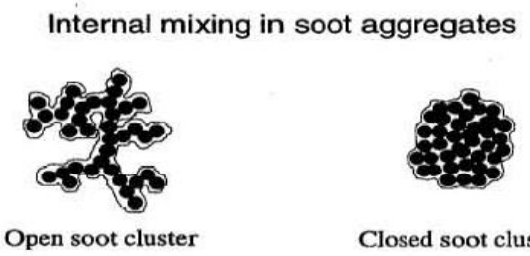

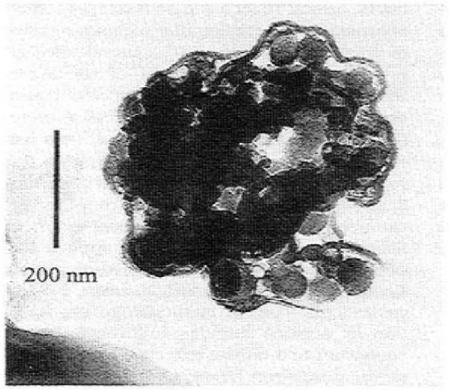

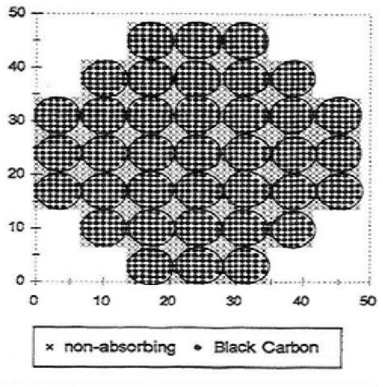

Light Absorption & Scattering by BC / Dust

BC: Highly Absorbing
Dust: Absorbing & Scattering

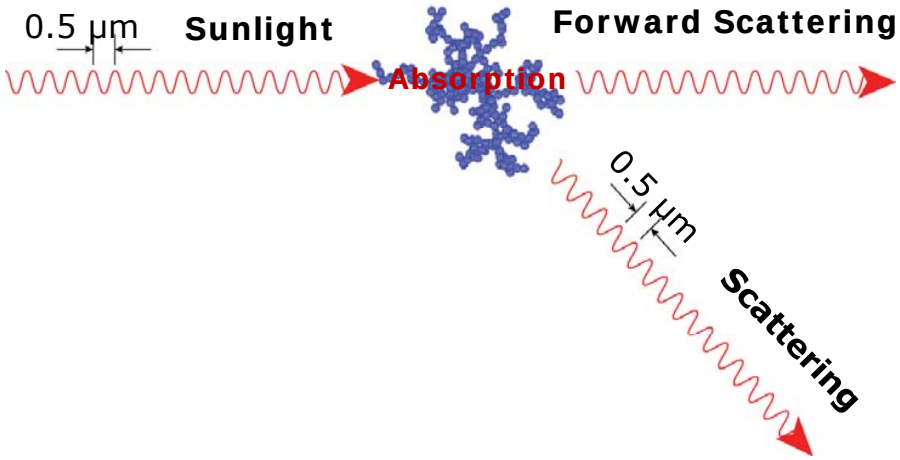

Absorption: Transform to Heat

Scattering: Redirect the energy in different directions

Direct Radiative Forcing & Regional Climate

Absorption of Sunlight by BC / Dust

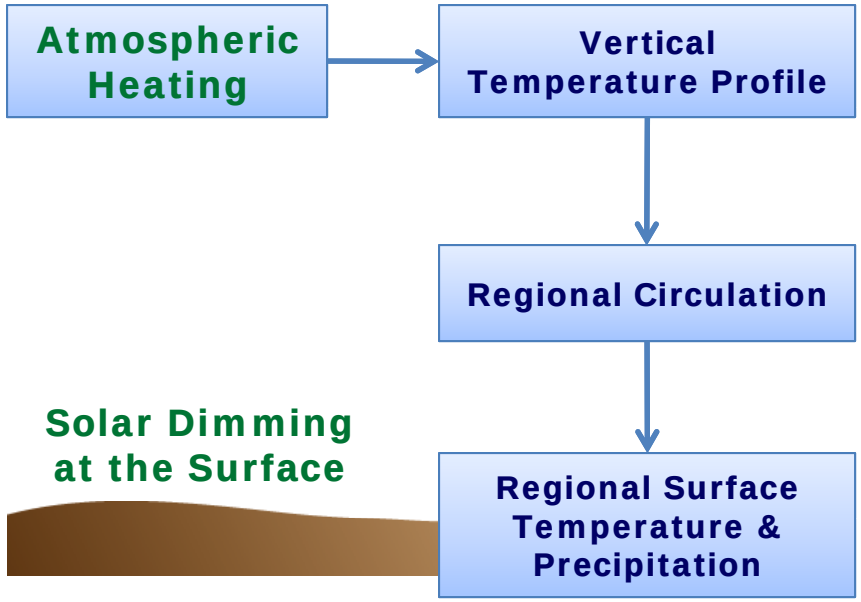

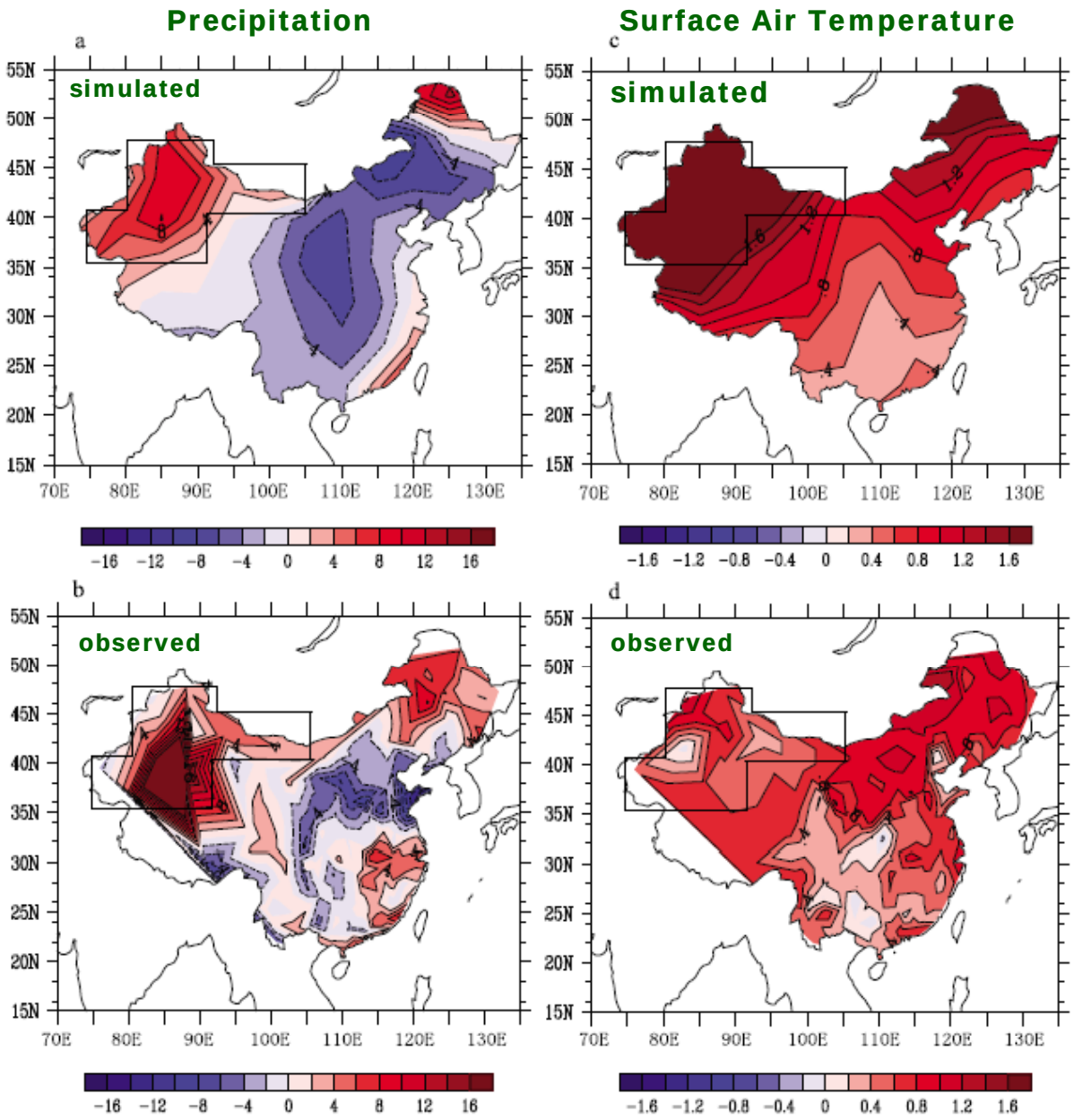

Simulated annual mean differences in (a) precipitation (%) and (c) surface air temperature (K) between Experiments B and A, along with the observed (b) precipitation (%) and (d) surface air temperature anomalies (K) over China in the1990s. Exp A consists of 10% BC and 90% non-absorbing aerosols (ω = 0.92). Exp B consists of 15% BC and 85% 0f non-absorbing aerosols (ω =0.88). The sea surface temperature, greenhouse gases, and other forcings are fixed in these two experiments so that aerosols are the only forcings in 5-year simulations (after Gu, Liou et al. 2010).

Construction of aggregates based on stochastic processes using homogeneous and shell spheres (smooth and irregular) as building blocks (Liou et al. 2010, 2011): closed and open cells, and observed soot.

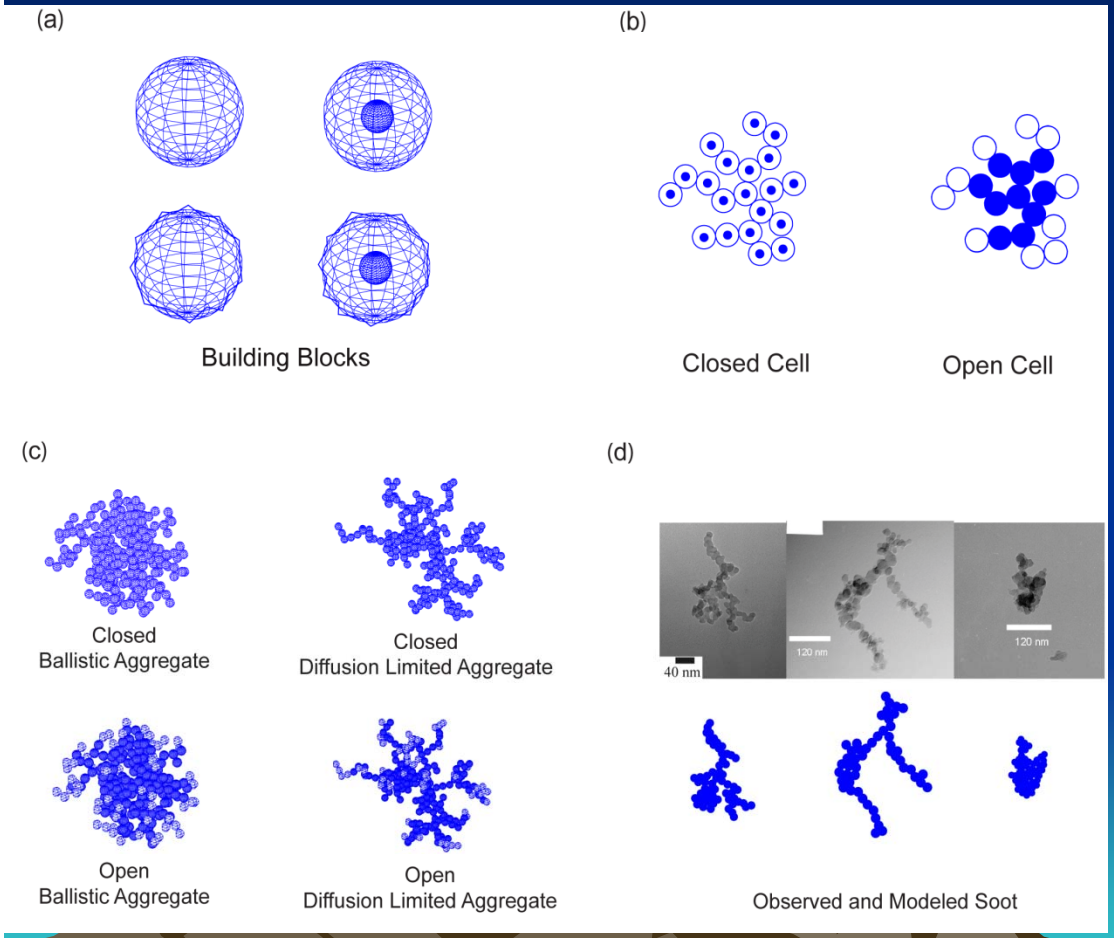

Light absorption and scattering by small irregular particles based on the geometric-optics and surface-wave approach verified by comparison with existing results for columns and plates (Liou, Takano and Yang 2011).

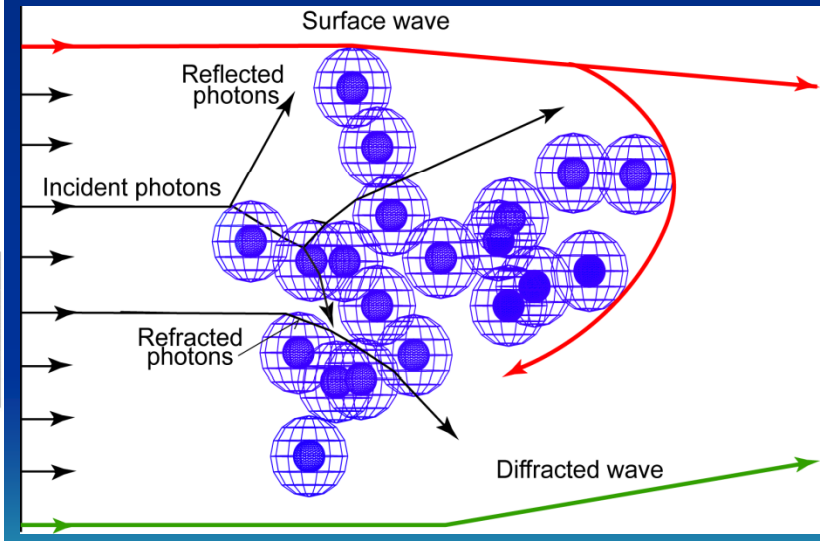

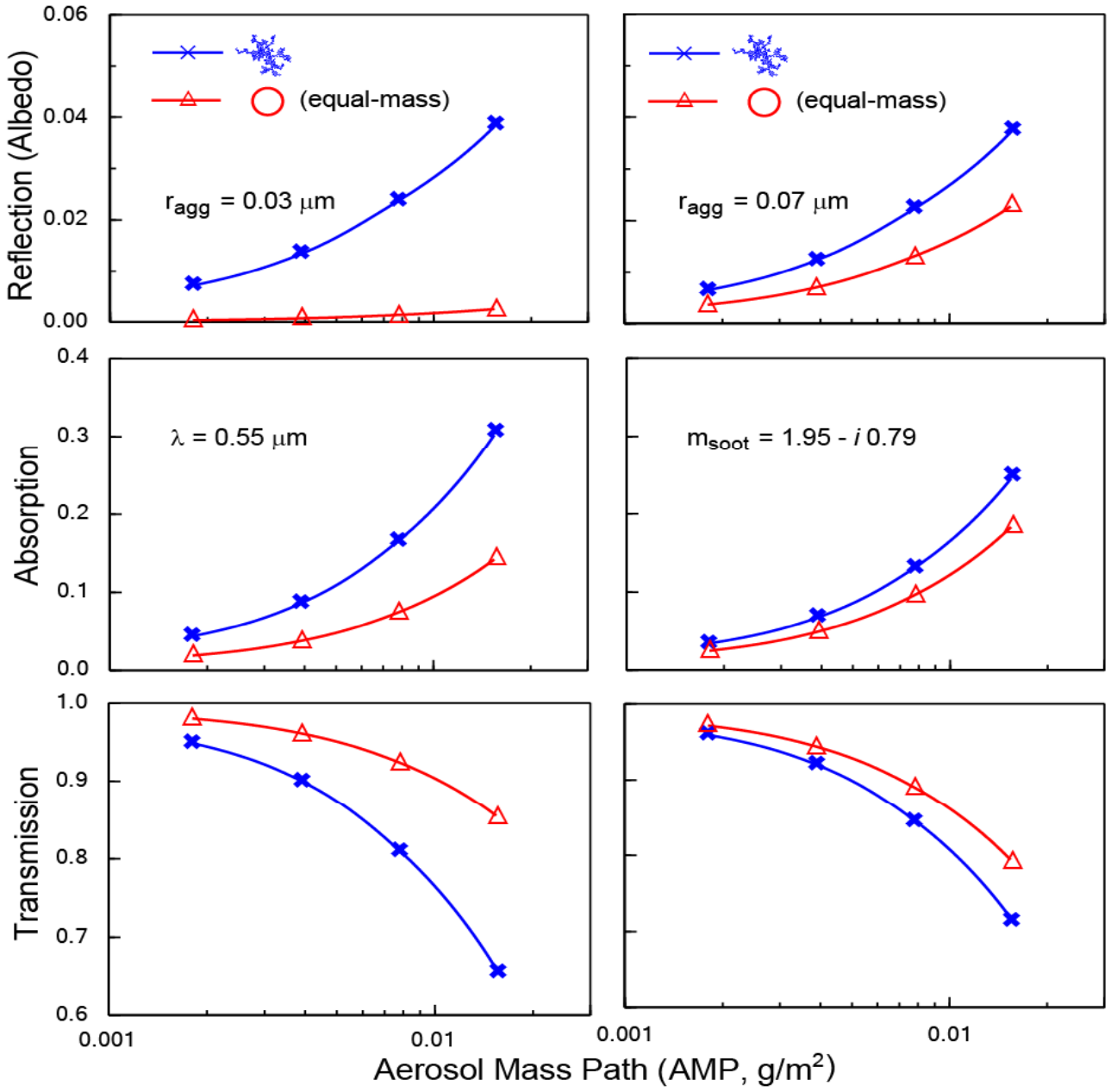

Reflection (Albedo), absorption, and transmission for a soot layer as a function of aerosol mass path (AMP) on a black surface using a solar zenith angle of 60^0. The 0.03 μm radius is the mean observed equivalent radius for BC aerosols. See substantial differences between the two BC shapes using diffusion limited aggregate and equal-mass (and equal-volume) spheres. Optical depth τ can be obtained by τ = a_e AMP, where a_e is the specific extinction coefficient (m^2/g). The adding-doubling method was used for radiative transfer calculations.

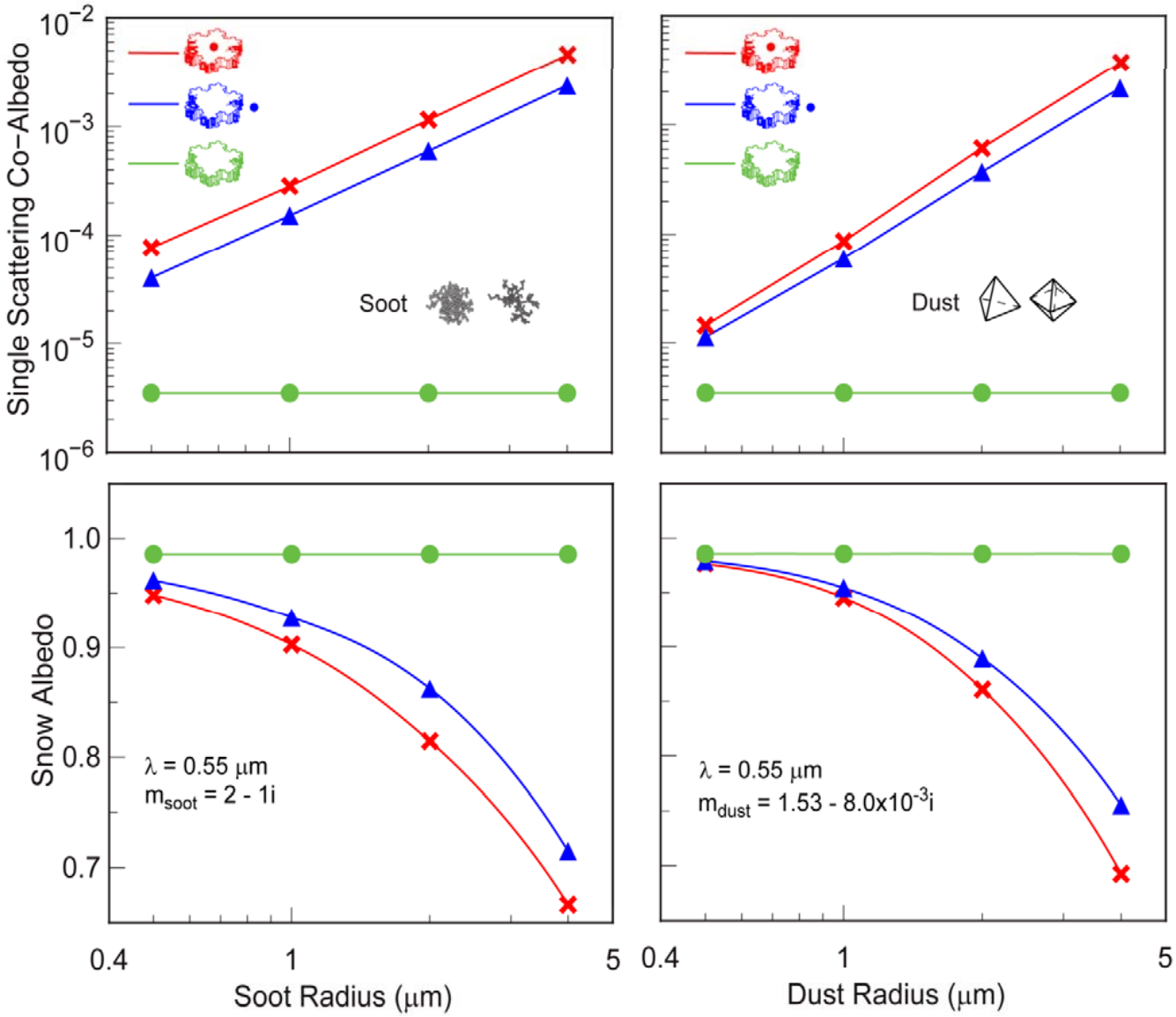

Visible single-scattering co-albedo (the ratio of absorption and extinction coefficients) and snow albedo as a function of soot and dust equivalent radii for a snow grain of 50 μm in equivalent radius for pure and contaminated conditions (μ_0 = 0.5 and optically semi-infinite snow layer). Large differences in snow albedo are shown with external and internal mixing cases. A 1 μm soot particle internally mixed with snow grains could effectively reduce snow albedo as much as 5-10 % (Liou et al. 2011).

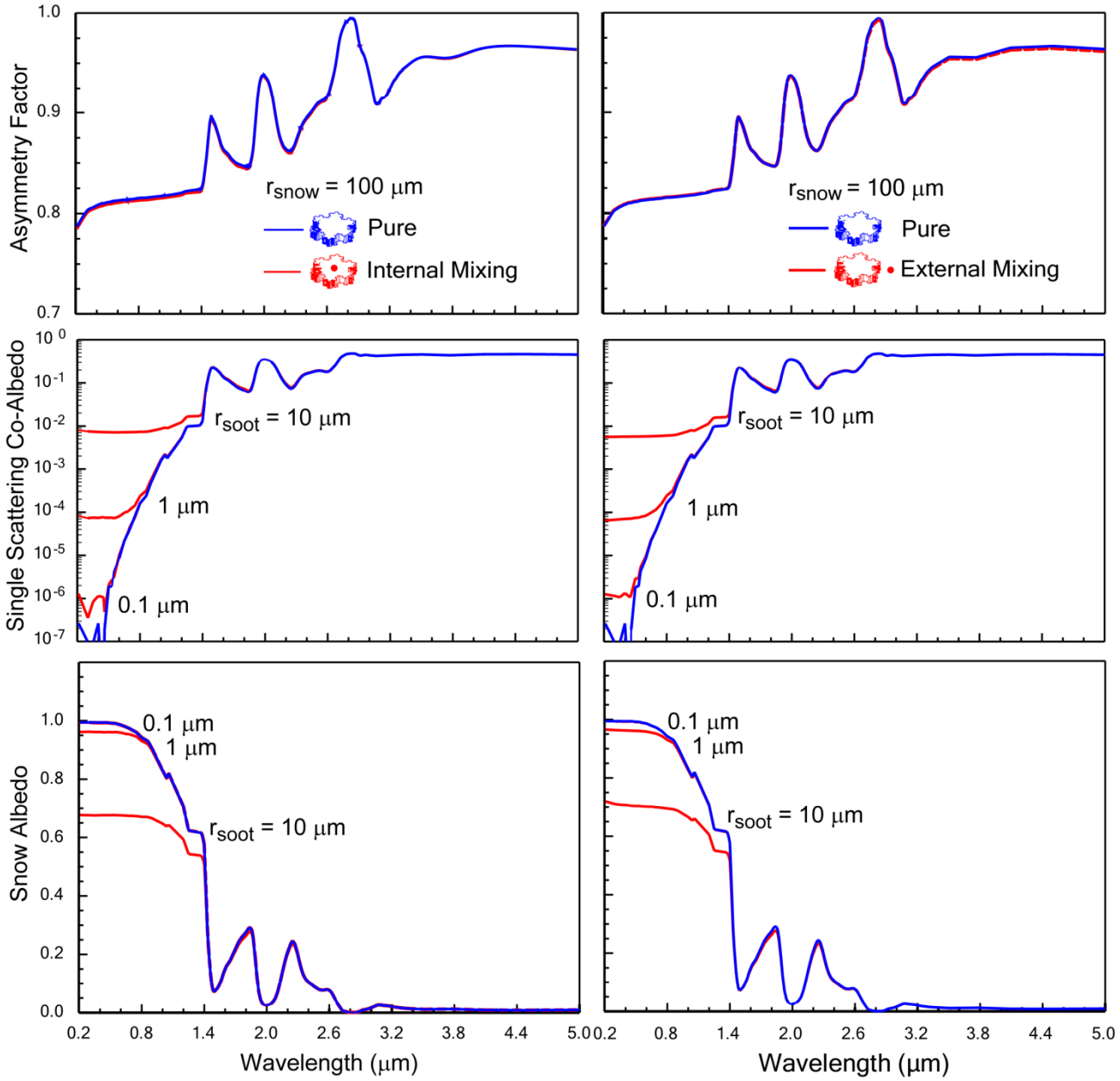

The effect of internal and external mixings in snow grains on spectral snow albedo (0.2-5μm) for μ_0 = 0.5. The snow grain size is 100 μm with 3 BC sizes of 0.1, 1, and 10 μm. The refractive indices of ice and BC were taken from Warren and Brandt (2008) and Krekov et al. (1993), respectively. Upper panel: Asymmetry factor. Middle panel: Single-scattering co-albedo. Lower panel: Snow albedo for an optically semi-infinite layer. For application to CLM-WRF, total BC deposition can be converted to a mean BC size.

3D Radiative Transfer (Monte Carlo Photon Tracing) in Mountains: 10-30 W / m² in Regional Surface Energy Balance (Liou et al. 2007; Lee et al. 2011, regression parameterization for use in WRF-CLM)

Solar radiation:

- Direct: solar incident angle θ_i
- Diffuse: sky view factor V_d
- Direct reflected: terrain configuration factor C_t
- Diffuse reflected: terrain configuration factor C_t
- Coupled: terrain configuration factor C_t

Thermal infrared radiation:

- Emitted in the atmosphere or from the surface
- Starting location sampled from a set of pre-divided cubic cells
- Random direction and isotropic emission (emissivity & temperature)

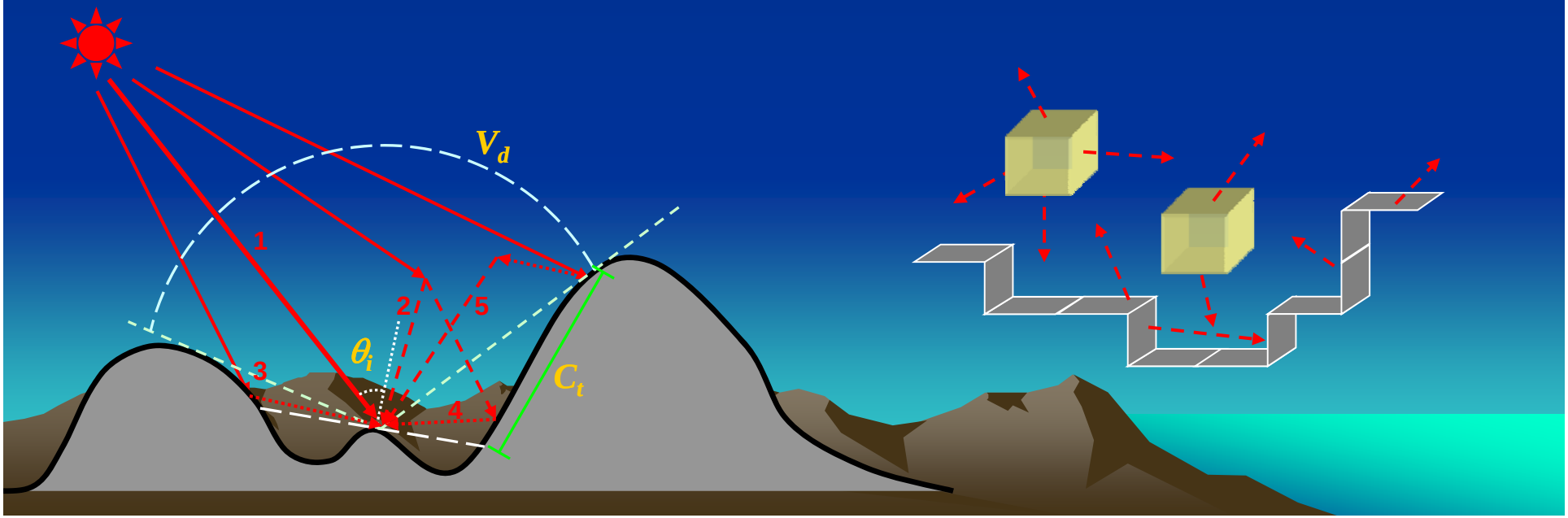

Differential Equation for Land Surface Temperature

$$C_{ps}\, dT_s / dt = F_S + F_{IR} + F_H + F_{IS}$$

where C_{ps} is the surface heat capacity; t is time; F_s, F_{IR}, and F_H represent net solar, longwave, and heat fluxes at the surface, respectively; F_{IS} denotes fluxes associated with ice/snow melting. With reference to a flat surface, **3D mountain effects can produce 10-30 W/m² differences in solar fluxes in 30x30 km² domains (Liou et al. 2007)**

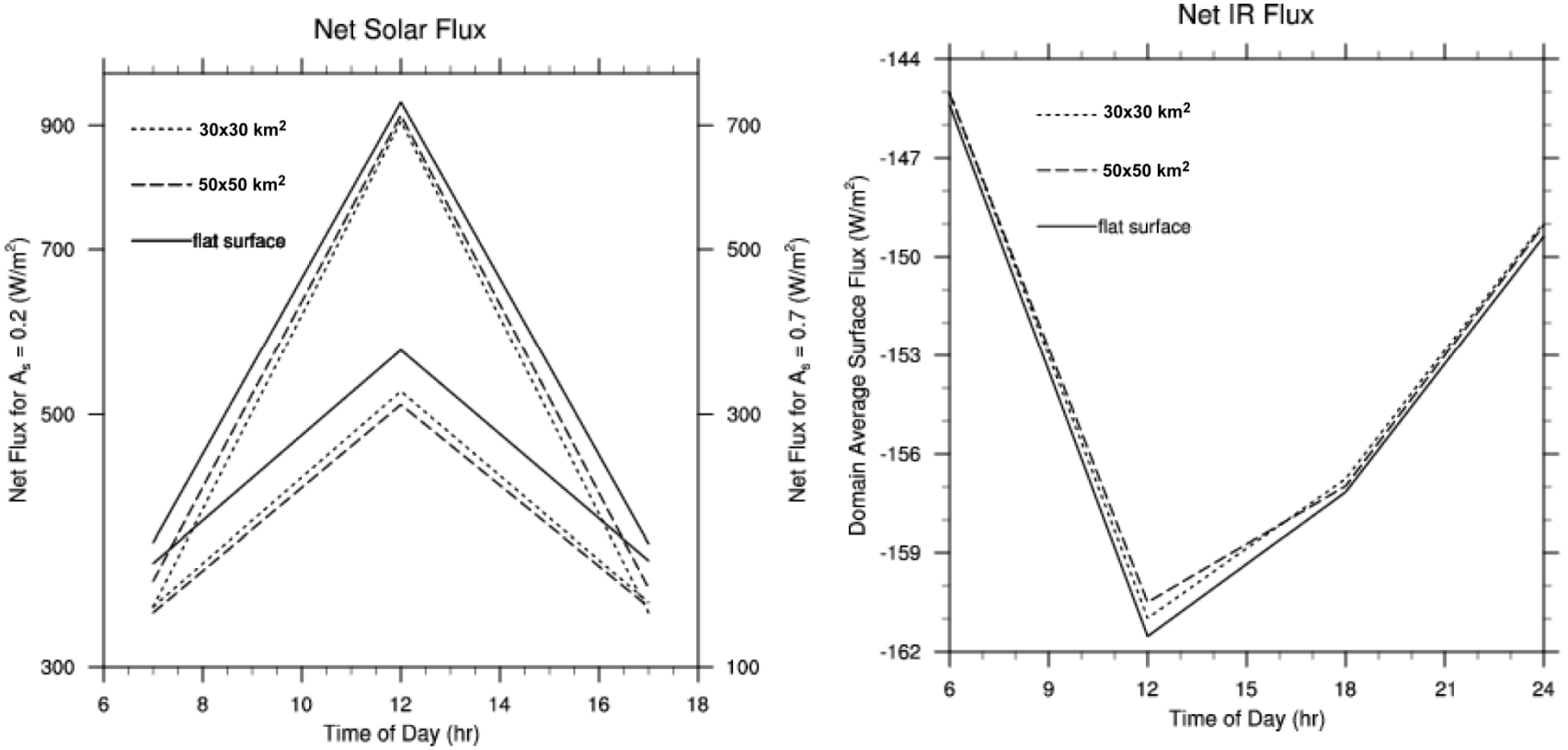

Differences between the domain-averaged net radiative flux on mountains and a flat surface as a function of time of day using surface albedo values of 0.2 and 0.7 for two domains of 30×30 km² (centered at Lhasa, Tibet) and 50×50 km² on March 21 (equinox).

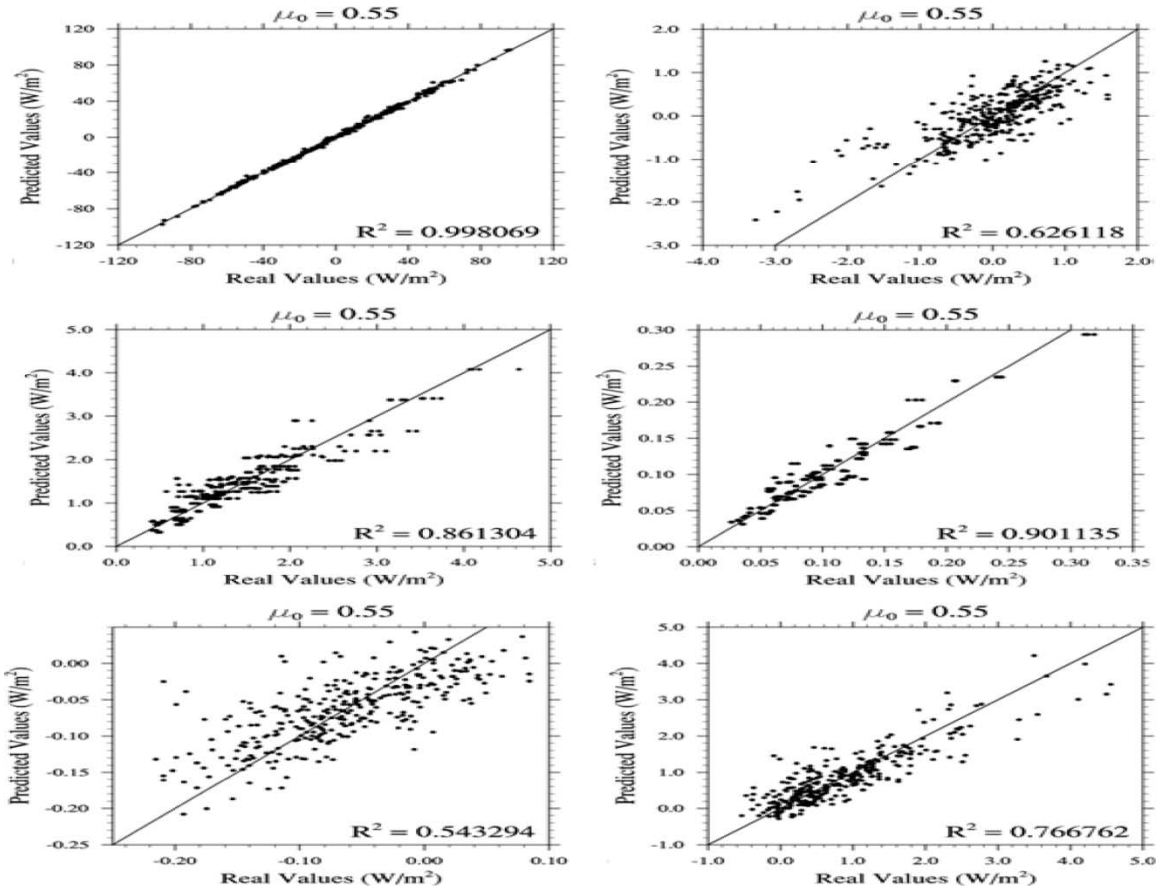

Comparison of the deviations of the five flux components computed from Monte Carlo simulations (real values) and multiple regression equations (predicted values). The upper panel is for direct (left) and diffuse (right) fluxes. The middle panel is for direct-reflected (left) and diffuse-reflected (right) fluxes. The lower panel shows the coupled flux with a surface albedo of 0.1 (left) and 0.7 (right). The most important component is direct flux (~ 700 W/m²), followed by direct-reflected flux (Lee et al. 2011).

We have derived 5 universal regression equations for flux deviations which have the following general form:

$$F^*_i = a_i + \Sigma\, b_{ij}\, y_j,\ i = \text{dir, dif, dir-ref, dif-ref, and coup,}$$

where a_i is the intercept, y_j is a specific variable, and b_{ij} are regression coefficients. For example, for the deviation of direct flux, we have $F^*_{dir} = a_1 + b_{11}\, y_1 + b_{12}\, y_2$, where y_1 is the mean cosine of the solar zenith angle and y_2 is the mean sky view factor. This parameterization is applicable to clear as well as cloudy conditions using cloud optical depth as a scaling factor.

3D Mountain/Snow & Absorbing Aerosols: A Combined Regional Climate System

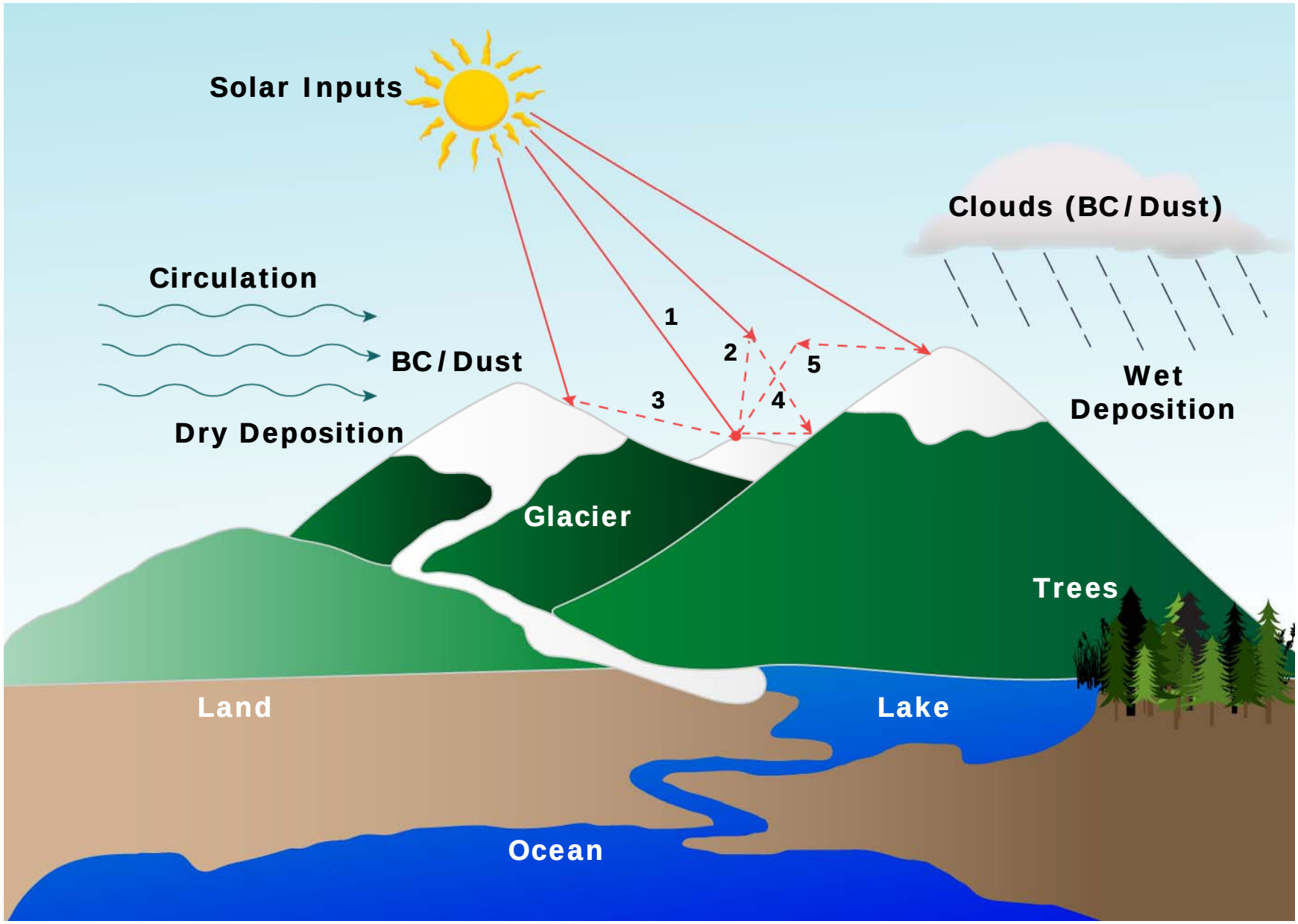

An Illustration of Mountain/Snow-Albedo Feedback due to Absorbing Aerosols

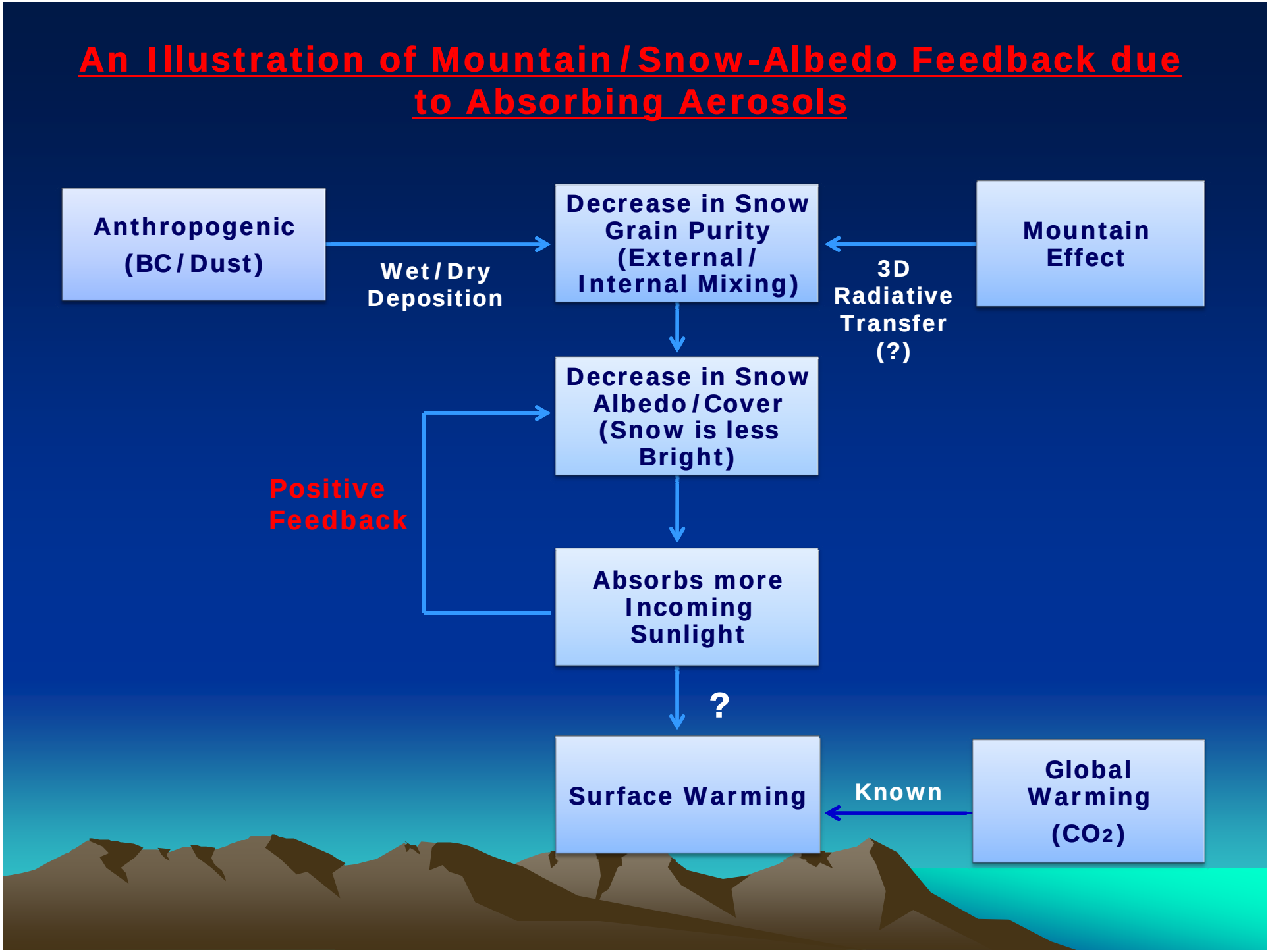

Human and Natural Drivers of Climate Change

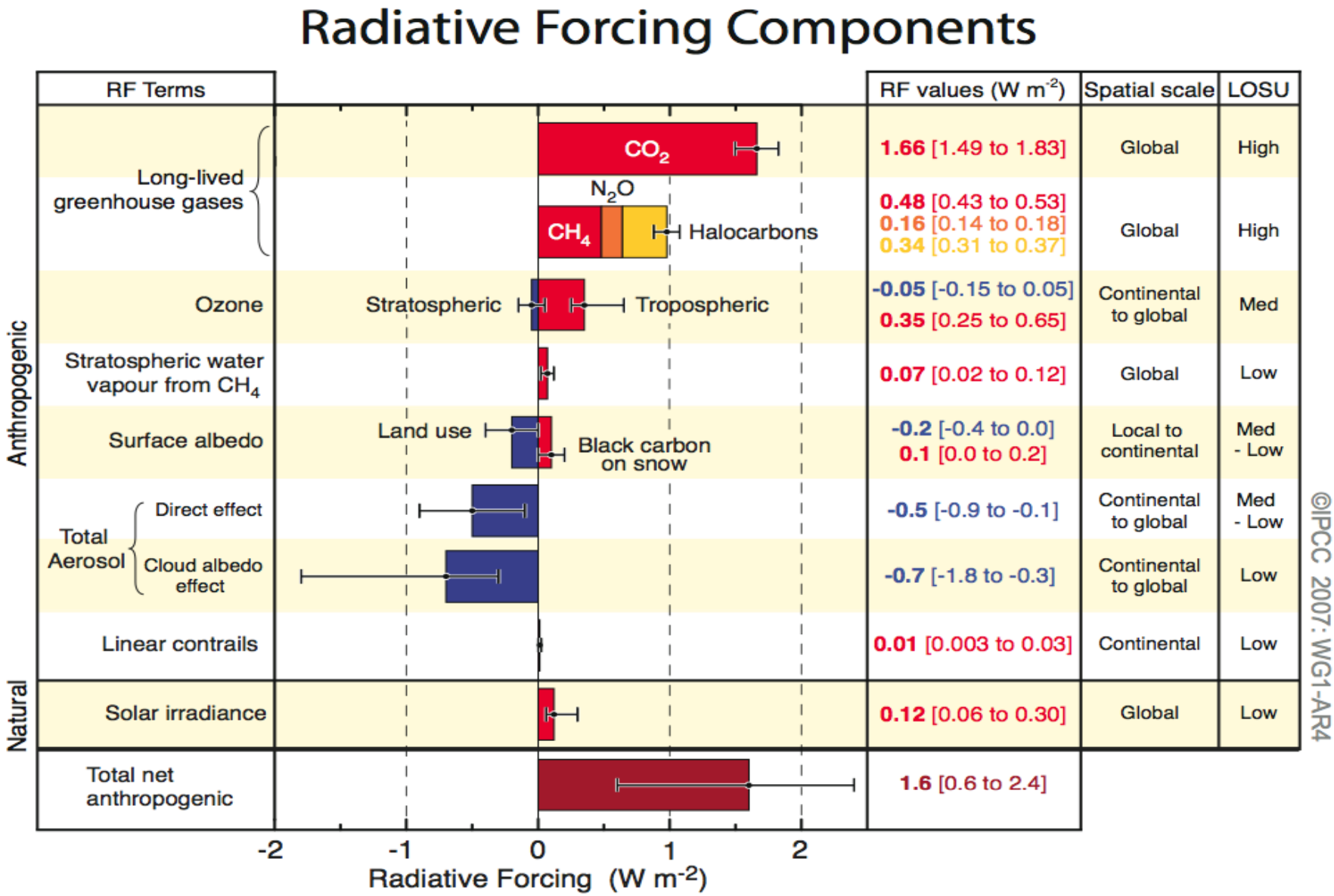

Connection to Surface Energy Balance Equation (Community Land Model, CLM <-> WRF)

Basic Equation

$$(\bar{S}_g + \bar{S}_v) + L^{\downarrow}_{\text{atm}} - L^{\uparrow} - (H_v + H_g) - (\lambda_{\text{vap}} E_v + \lambda E_g) = G$$

G = Ground Heat Flux $(= \partial T_S / \partial t)$

$(\bar{S}_g + \bar{S}_v)$ = Absorbed Solar Flux (v = vegetation, g = ground): 3D Effect

$L^{\downarrow}_{\text{atm}}$ = Incident Longwave Flux: 3D Effect

$L^{\uparrow}$ = Emitted Longwave Flux: 3D Effect

$(H_g + H_v)$ = Sensible Heat Flux

$(\lambda_{\text{vap}} E_v + \lambda E_g)$ = Latent Heat Flux (λ = certain coefficient)

3D Mountain Effects

$S_o(\text{3D}, \alpha)[1 - \alpha(\text{snow})]$; S_o = Incident Solar Flux, α = Snow Albedo

Solar Direct & Diffuse Beam (Visible & Near-IR): 3D Monte Carlo and Plane-Parallel Radiation Parameterizations

External & Internal Mixing of BC in Snow Grains

α(Grain Size, BC) = Snow Albedo: Optical Depth, Single-Scattering Albedo & Asymmetry Factor

Effects of Climate Change on California: A Research Frontier

- Precipitation and snow distribution (mountain ecosystems, ski industry)
- Water resources and management
- Santa Ana events (human health, wildfire)
- Runoff/streamflow (coastal wetlands)
- Sea surface temperatures (ocean ecosystems)
- A JIFRESSE mission: Building a regional climate model to include 3D mountains/snow and absorbing aerosols for process studies, physical understanding, and climate projection